HYDRAULIC CHARACTERISTICS OF ROCKFILL DROP STRUCTURES

by

Ernest Bruce Webb

A thesis
presented to the University of Manitoba
in partial fulfillment of the
requirements for the degree of
Master of Science in Civil Engineering
in
The Faculty of Graduate Studies

Winnipeg, Manitoba, 1983

THE UNIVERSITY OF MANITOBA

FACULTY OF GRADUATE STUDIES

The undersigned certify that they have read a Master's thesis

entitled: ....Hydraulic Characteristics of Rockfill Drop.........

........Structures...

....

submitted by ....Ernest Bruce Webb..............................

in partial fulfillment of the requirements for the degree of

........MASTER OF SCIENCE..

The Thesis Examining Committee certifies that the thesis

(and the oral examination, if required) is:

Approved ☑   Not Approved ☐

....
Advisor

....

....

....

....
External Examiner

Date ...12./Dec./83...............   ....

HYDRAULIC CHARACTERISTICS OF ROCKFILL DROP STRUCTURES

BY

ERNEST BRUCE WEBB

A thesis submitted to the Faculty of Graduate Studies of
the University of Manitoba in partial fulfillment of the requirements
of the degree of

MASTER OF SCIENCE

©ᵛ 1983

ABSTRACT

The purpose of this study was to investigate the hydrau-
lic characteristics of rockfill drop structures modelled on
those located on Wilson Creek near the Wilson Creek Experi-
mental Watershed on the Manitoba Escarpment. These struc-
tures were designed to reduce the slope of the streambed
through an erodible alluvial fan in order to reduce the dep-
osition of shale on farmland below the fan. In addition to
examining the hydraulic performance of the individual struc-
tures with physical models, changes to the geometry of the
structures were studied to determine the effect of down-
stream slope and crest cross section. The structures tested
were stable well beyond the design discharge. Little dif-
ference was found between the performances of structures
with downstream slopes of 20:1 and 15:1. It was found that
a sharp crested weir was a suitable model for approximating
the hydraulic performance of the structures tested. The ef-
fect of several changes in physical model design were also
investigated. Further tests are required to isolate the ef-
fects of roughness and permeability on the model structures.

Following the physical model tests of the individual
structures, a mathematical model of a series of two drop
structures was used. The result of this testing with the

HEC-2 backwater model indicated that the structures can only be effective if the backwater effect from one weir extends to the next upstream weir. Furthermore, the infilling of the pools above the structures with sediment does not significantly affect the hydraulic performance of the weirs.

ACKNOWLEDGMENTS

which have substantially improved the text of this thesis. The finished form of the manuscript as well as much of the preparation of earlier drafts was made possible by the word processing skill of David Webb.

Special thanks are due to Professors Cass Booy of the Civil Engineering Department and Allan Trupp of the Mechanical Engineering Department for their reviews of the thesis on behalf of the Faculty of Graduate Studies.

Finally, the contribution of Professor Luis Magalhaes is gratefully acknowledged. His interest, expertise, patience and friendly persistence guided this study on its long course from concept to completion.

CONTENTS

LIST OF FIGURES

LIST OF PLATES

Plate

NOMENCLATURE

a	Acceleration
B	Weir crest width
b	Bottom width of trapezoidal chute
C_D	Drag coefficient
D	Depth of flow; depth of chute
D_t	Tailwater depth
d	Diameter of particle
d_m	Median particle diameter
d_{50}	Particle diameter at which 50% of material by weight is finer
E	Elasticity
F	Force
Fe	Elasticity force
Fg	Gravity force
Fi	Inertial force
Fp	Pressure force
Fr	Froude number
Ft	Surface tension force
Fv	Viscosity force
F_B	Force acting on a single particle
F_D	Drag force
F_d	Form drag

F_v	Viscous drag
g	Acceleration due to gravity
H	Horizontal; head on weir
K	Grain size
L	Length
m	Mass
m	Model quantity (Subscript)
n	Manning number
p	Pressure
p	Prototype quantity (Subscript)
Q	Discharge
q	Discharge per unit width (unit discharge)
R	Hydraulic radius
Re	Reynolds number
Re*	Particle Reynolds number
S	Slope
SS	Side slope
S.F.	Safety factor
S_o	Bed slope
S_s	Specific density of solid material
T	Time
V	Vertical
v	Velocity
v*	Shear velocity
vol	Volume
α	Angle between bed and horizontal plane
γ	Unit weight of water

γ_s	Unit weight of solids
η	Value proportional to Shields Entrainment Function
θ	Angle of V notch weir
λ	Scale ratio (general)
λ_F	Force scale ratio
λ_H	Horizontal length scale ratio
λ_L	Length scale ratio (general)
λ_T	Time scale ratio
λ_V	Vertical length scale ratio
μ	Dynamic viscosity
ν	Kinematic viscosity
ρ	Density of water
ρ_s	Density of solid material
σ	Surface tension
τ	Shear stress
τ_c	Critical shear stress
τ_o	Average bottom shear stress
ϕ	Angle of repose of non-cohesive material

Chapter I

INTRODUCTION

1.1   THE WILSON CREEK WATERSHED

The Wilson Creek Watershed is typical of many small wat-
ersheds on the eastern side of the Manitoba Escarpment in
terms of geomorphology and hydrology. Due to the small size
of the watersheds and their rapidly varying topography, the
highest streamflows are generally caused by intense summer
storms.   The eastern side of the escarpment is subjected to
high-intensity storms more frequently than any other part of
Manitoba. Streamflow produced by these storms may be two or
three orders of magnitude above minimum flows.   The upper
portion of the Wilson Creek Watershed receives 20 - 40% more
precipitation than the lower plains (Planning Branch, 1977,
1979).

Large amounts of sediment are transported during high
flow events due to the easily erodible nature of the shale
material which the streams flow through and the steep bed
gradients on the escarpment.   The sediment is deposited at
the foot of the escarpment in alluvial fans.   Farmland be-
yond the fans is subject to flooding and shale deposition
which damages or destroys crops and reduces the fertility of

the soil. Drains built to carry water off the farmland continually fill with sediment. The problem becomes more severe with time, since overflows become more frequent as the drains and main channels fill with sediment.

Wilson Creek has formed a large alluvial fan and continues to deposit substantial amounts of sediment at the downstream end of the fan. As may be seen in Plate 1, a canyon 10 - 15 m deep has been cut through the fan by the stream, leaving exposed shale banks which are easily eroded. Most of the sediment being deposited on fields downstream now originates in the fan itself rather than on the escarpment.

Water management problems have been made more serious by poor land use practices on the escarpment and the lower plains. Higher parts of the escarpment were set aside as timber reserves between 1896 and 1906. At the time, settlers preferred more easily farmed land away from the escarpment (Carlyle, 1980). In 1908, settlement began on land immediately below the escarpment. By 1916, the provincial government began to construct artificial drains to relieve drainage problems in the newly settled areas (MacKay, 1969). Sedimentation problems were noted in these drains as early as 1921 (Carlyle, 1980). The drains collected and channelized water which had previously spread across the alluvial fan. This flow concentration in the easily eroded fan entrained large amounts of sediment which were then deposited in the new drains below the fan.

Administration of land was made a provincial responsibility in 1930. At the same time, Riding Mountain National Park was created. Timber cutting and grazing was still allowed at this time. In 1949 the joint federal-provincial Northwest Escarpment Agreement was reached. This agreement provided for cost-shared relief programs to solve the problems of scarpface erosion and lowland flooding along the Riding, Duck, and Porcupine Mountains.

Flood control reservoirs are commonly used to reduce flood discharges on streams. Water is retained in the reservoir until after the peak flow has passed and is then slowly released when the streamflow has decreased. This concept of headwater control led to the development of two reservoirs in the headwaters of the tributaries to Wilson Creek. By reducing flood peaks, some downstream erosion/ deposition problems were reduced. The provision of reservoirs proved to be a very expensive solution to the problems in the watershed; none have been built in recent years.

A joint federal-provincial committee on Headwater, Flood and Erosion Control was formed in 1957. The Wilson Creek Watershed was selected as a study area to gather pertinent data and test alternative solutions to the various problems along the eastern side of the Manitoba Escarpment. The study started in 1959 and has continued to the present (Planning Branch, 1979). Since 1959 a large amount of hy-

drological and meteorological data has been collected. This data has proved useful for forecasting floods (Carlyle, 1980; Strilaeff, 1976). In addition to data collection, several experiments on sediment measurement and control have been conducted. The general layout of the watershed in Western Manitoba is shown in Figure 1.1.

The land on the plains below the escarpment has been the object of a federal-provincial land acquisition program since 1962. Following purchase, cultivated land has largely been sown to forage crops. This increases soil fertility and reduces erosion by reducing runoff. Steeply sloping land has been reforested (Carlyle, 1980).

Despite these non-structural measures, work has continued on direct methods to reduce erosion along the fan. Bank protection and gradient control are two common methods of reducing the potential for erosion on streams. Bank protection, while effective for relatively short reaches, is prohibitively expensive for channels such as that of Wilson Creek and the other streams on the Escarpment. In addition to the length of protection required, the banks are generally very steep, and may be almost vertical in many locations. Bank protection is therefore not a practical solution to reducing erosion problems in this type of channel.

1.2   CHANNEL PROTECTION BY GRADIENT CONTROL

The value of the land to be protected is a significant constraint on the design of structural relief measures to reduce flood and sediment damages. Although much of the land along the downstream reaches of Wilson Creek is cultivated, it is of relatively low value. Conventional concrete drop structures are too expensive for use in such a situation. As an alternative, the Water Control Works Section of the Manitoba Water Resources Branch has proposed a series of rockfill weirs along the reach of the stream within the alluvial fan as an experiment to reduce the gradient of the stream and hence its erosive power. Each of the five proposed structures is less than 2 m in height; in total, 8.5 m of head is dissipated in a length of about 1.38 km. In this way, the gradient is reduced from 0.0095 to 0.0033. The general layout of the structures is shown in Figure 1.2, and the bed profile along the same reach is shown in Figure 1.3.

The design discharge used in the proposed solution is 24 m^3/s, which corresponds to a 10% frequency of exceedence of maximum instantaneous summer flow or a 2% frequency of exceedence of maximum mean daily flow. The maximum recorded discharge on Wilson Creek was 45 m^3./s during the storm of October 1975 (Planning Branch, 1979).

A rockfill structure was chosen to make use of locally available rock which could be obtained and placed at rela-

tively low cost. To reduce the probability of piping under the weirs, a membrane consisting of railway ties fastened with steel angles was designed. Although this membrane is permeable, it was felt that it would at least serve as a cantilever retaining wall under the most critical conditions. The probability of piping after the pool was filled with sediment was considered small, so the membrane was included only to protect the structure for the first few years.

The structure itself consists of a wide shallow chute in the central area of the stream cross section with higher shoulders on either side to concentrate the flow in the center of the stream. A cross section through the crest of a typical weir is shown in Figure 1.4 and a typical weir profile is shown in Figure 1.5. The chute floor is 0.75 m lower than the shoulders. The expected depth of flow at the design discharge is 0.45 m, with 0.3 m freeboard. Both the chute and shoulders have a longitudinal slope of 20:1. The crest width of 18 m and the 20:1 slope were chosen so that locally available rock would be stable. For the upstream weir, a more narrow natural channel cross section resulted in a reduction of the designed chute width to 12 m with an increase in depth to 0.9 m. A 25:1 longitudinal slope was recommended for this structure.

The stone size specification chosen for the design was 15% by count between 0.68 m and 0.45 m and 85% between 0.45 m and 0.10 m. The d_{50} value of this specification is approximately 0.24 m.

The design required some excavation at the toe end to allow placement of a short rock transition section; no stilling basin was provided.

The first two structures at the upstream end of the reach were constructed during the fall and winter of 1980-1981. Plates 2 - 6 show the structures in the early spring of 1981 and in August, 1981.

The Civil Engineering Department of the University of Manitoba was approached to undertake a hydraulic model study to examine aspects of the hydraulic performance of the structures. Of particular interest were the hydraulic characteristics of the weirs, the stability of the structures, and the effects of the structures on the flow characteristics of the stream. These aspects were studied in conjunction with other features of more academic interest. These interests included changes to the geometry, roughness and permeability of the structures as well as the effects of scale distortion on structural hydraulic models.

All tests made use of simplified geometries. In addition to reducing the complexity of the system to be modelled, the

simplification also made the results of the study more general and thus more applicable to different locations.

1.3 SCOPE OF STUDY

Investigation of the proposed structures involved two types of models. A physical model was used to study the hydraulic characteristics and stability of the individual structures while a mathematical model was used to examine the effect on depths and velocities in the stream.

Chapter II provides background on rockfill and rockfill drop structures. Reasons for using rockfill rather than concrete are discussed and theoretical aspects of stone stability are considered. In addition, the design proposed for the Wilson Creek Weirs is checked against design criteria developed by Smith (1978) at the University of Saskatchewan.

The third chapter discusses the theory of hydraulic models. After an examination of the requirements for similitude between prototype and model, distorted and undistorted models are studied. Both types were used in the physical model testing program.

The fourth chapter describes the experimental work done in both the physical and mathematical model testing programs. The design and operation of the various physical models is explained in detail. The mathematical modelling

component utilized the well known HEC-2 backwater model. Due to the length and complexity of this program, only a brief description is provided of input information and model results.

In the fifth chapter, all model results are analysed and discussed. A single structure prototype rating curve is developed from the physical model tests and the stability of the structures and their failure mode is examined. Many changes to the geometry of the structures were tested with the physical models. These changes were made in an attempt to assess the effect of design changes on the structures. Among the changes studied were changes in weir profile, chute cross section, rock size, and permeability. The effects of model distortion and scale changes were also studied. Three sets of tests were made with the HEC-2 model. Six discharges were used in each series, ranging from one quarter to twice the design discharge of 24 m^3/s. The first series of tests was run in a simplified channel without any structures. This series attempted to reproduce "natural" conditions. The second series tested the same channel section with two structures included. In the third series, the pools upstream of the structures were assumed to be full of sediment to the crest level of the weirs. The results of all three series of tests are examined to determine possible changes to the regime of the stream after the installation of the structures.

Conclusions and recommendations are presented in Chapter VI.

Chapter II

ROCKFILL

2.1   GENERAL CONSIDERATIONS

Rockfill can be placed at a much lower unit cost than concrete. The saving is particularly significant for small structures in remote locations. Rock is widely available in a variety of sizes. It is easily handled and may be placed by dumping with a minimum of labour. In less developed areas, inexpensive labour may be substituted for machinery; little skill is required for placement. Construction is rapid and requires little site preparation.

Because rockfill contains relatively large voids, more volume is required for the same mass as an equivalent concrete structure. This is because rockfill has a typical bulk density of 1700 kg/m^3 while concrete has a bulk density of 2400 kg/m^3. In addition, the loadbearing capability of rockfill is much less than that of concrete. Rockfill therefore would not be used in hydraulic structures requiring heavy components such as piers. Despite these potential drawbacks, rockfill may be used in many structures in place of concrete. For poor foundation conditions, rockfill may be preferable to a rigid concrete structure. Three particu-

lar hydraulic advantages of rockfill may be especially sig-
nificant.

In concrete structures uplift requires costly drainage
and cutoff provisions; in rockfill uplift is not a problem.
In addition to permitting upward flow, the permeability of
rockfill allows additional flow through the structure as
shown in Figure 2.1. Small flows may be conveyed through
the structure without overtopping the crest - this condition
is known as throughflow. The roughness of the surface as-
sists in the dissipation of surplus energy in two ways. In
addition to friction between the rocks and water, energy is
dissipated by jet impingement as the water flows over and
through the rock layers (Stephenson, 1979).

In cases where both throughflow and overflow occur, the
throughflow portion of the total discharge is relatively
small (Olivier, 1967). Throughflow is also reduced if the
voids fill with sediment or debris. This may become a seri-
ous problem for structures designed for throughflow only,
since the point where the flow breaks out on the downstream
slope will rise. In an improperly designed structure, if
the breakout point rises into a steeper upper slope, that
slope may become unstable.

A horizontal crest is important for rockfill structures
which will be overtopped. If the crest is not levelled,
flow concentration will occur. This may lead to gullying on

the downstream slope of the structure which will further concentrate the flow and may cause a complete washout of the structure. A rigid crest may be used to protect the structure against this possibility. A membrane extending to the crest will serve the same purpose while making the structure impermeable to the crest height.

2.2 STABILITY OF STONES

Stones on a rockfill structure must resist a combination of turbulent drag and lifting mechanisms. Movement takes place by sliding rather than overturning, since for minimum energy requirements, the representative vertical dimension of the rock is less than the representative horizontal dimension. This causes a non-spherical stone to lie "flat". (Stephenson, 1979).

The stone size required to resist movement may be determined with the Shields Criterion (Smith, 1978). In order to see how this may be done, the stability of a single stone may be considered.

The mass forces acting on a single stone resting upon a horizontal bed of non-cohesive material are:

[2.1] $$F_B = gd^3(\rho_s - \rho)$$

where   g is the acceleration due to gravity

               d is the stone diameter.

              ρ is the density of water.

ρ_s is the stone density.

Under conditions of no flow there are no drag forces; the external force on the particle is equal to the submerged weight of the particle. This is also the force which will be available to resist motion. Under conditions of flow, drag is related to shear velocity. Shear velocity is related to the real fluid velocity which would produce a shear stress τ . Shear velocity is defined as follows:

[2.2] $\qquad v* = \sqrt{\tau/\rho}$ $\qquad \tau = V^{*2}\rho$

When flow over the particle is turbulent, form drag is the dominant force on the particle. Form drag may be defined as follows:

[2.3] $\qquad F_D = \rho d^2 (v*)^2$ $\qquad V^* = \sqrt{\dfrac{F_0}{\rho d^2}}$

$\qquad\qquad\qquad = \tau d^2$

When flow over the particle is laminar, viscous shear force dominates. This force (also known as viscous drag) may be defined as follows:

[2.4] $\qquad F_v = \mu d v*$ $\qquad V^* = \dfrac{F_v}{\mu d}$

where μ is the dynamic viscosity.

The particle Reynolds number indicates whether form drag or viscous drag is the dominant force on a particle. This parameter is dependent on the shear velocity as follows:

$$\text{particle Reynold's } \# \quad = \quad \frac{\text{shear velocity} \times \text{diameter}}{\text{kinematic viscosity}}$$

15

[2.5] $Re* = v*d/\nu$

    where ν is the kinematic viscosity.

The particle Reynolds number is the ratio of form drag to viscous drag forces.

    Since both form drag and viscous drag are related to the shear velocity, forces promoting motion and forces resisting motion may be expressed in a single ratio:

[2.6] $$\frac{\rho d^2 (v*)^2}{(\rho_s - \rho) g d^3} = \frac{\tau}{(\gamma_s - \gamma) d}$$

    The relationship between this ratio and the particle Reynolds number is shown in Figure 2.2 as the familiar Shields Entrainment Function. Particle motion impends when $\tau = \tau_c$.

    Average bottom shear stress is given by the expression

[2.7] $\tau_0 = \gamma R S_0$

    where R is the hydraulic radius

           S_0 is the bed slope.

    When the fluid is water and the specific density of the solid material (S_s) is 2.65, (a common value in most sand and gravel streams),

[2.8] $$\frac{\tau}{d\gamma(S_s - 1)} = 0.056$$

    where 0.056 is an experimentally derived coefficient.

Substituting Equation 2.7 for τ_o and simplifying:

[2.9] $$\frac{RS_o}{d(S_s-1)} = 0.056$$

$$\frac{\gamma R S_o}{d\gamma(S_s-1)} = 0.056$$

Replacing S_s with its value of 2.65 yields

[2.10] $$d = 11 \, R \, S_o$$

$R = 2 \, m$

$S_o = 0.01$

Then $d = .22 \, m = 22 \, cm$

This corresponds closely to Smith's equation for stable stone size:

[2.11] $$d = 10 \, D \, S$$

Smith uses the depth of flow D in place of the hydraulic radius; the two values are virtually identical for a wide channel. The 10% difference in coefficients arises from the rounding off of the experimental Shields entrainment function parameter (0.06 as opposed to 0.056).

Richardson et al (1975) give an additional equation which explicitly defines the factor of safety against stone movement for riprap on a sloping bed.

[2.12] $$S.F. = \frac{\cos(\alpha)\tan(\phi)}{\eta\,\tan(\phi)+\sin(\alpha)}$$
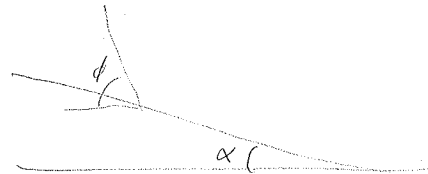
In this equation α is the angle between the bed and a horizontal plane and ϕ is the angle of repose of the riprap. For dumped riprap, the relationship between ϕ and mean particle diameter is shown in Figure 2.3.

η is proportional to the Shields Entrainment Function as follows:

[2.13] $\quad \eta = \dfrac{\tau_o}{(S_s-1)\gamma d}$

2.3 DESIGN CRITERIA

In addition to the stone size criterion given in Equation 2.11, Smith (1978) recommends the following criteria for the design of rockfill drop structures:

1) The minimum thickness of stone in the chute is 1.5 d_{50}. 50% of the stones by weight have a diameter less than d_{50}. This prevents the possibility of a void extending through the structure to the bed.

2) Graded rather than uniform stone is used to reduce the voids. This increases the unit weight and particle contacts while decreasing the porosity. The increase in unit weight improves stability; shear resistance is improved by additional particle contacts. The decrease in porosity is an asset because it may eliminate the need for a filter between the weir and the streambed.

3) At the downstream end of the chute, channel protection is necessary since flow leaving the chute will be supercritical and the tailwater will be subcritical. Smith recommends extending the stone past the end of the slope for a distance 6 D_t where D_t is the tailwater depth.

The Manning Equation is used to determine the rock size required for the chute of the structure. Smith (1978) uses the following equation to relate Mannings n to the median diameter d_m:

(handwritten: duck drawing in hydraulics vortex)

[2.14] $n = 0.049d_m^{1/6}$

The median diameter is approximately the same as d_{50}.

In most problems, the design discharge is known, and the stone size and bed slope are selected. Equation 2.11 determines the depth of flow once the area and hydraulic radius are calculated from the Manning Equation.

(handwritten margin notes: Smith, slope, stone, size, $d \sim 10 DS$)

In the following section, the design proposed by the Water Resources Branch for the Wilson Creek drop structures is checked against these criteria.

2.4   REVIEW OF WILSON CREEK DROP STRUCTURES DESIGN

Design parameters as selected by the Water Resources Branch were:

design discharge $Q = 24 \text{ m}^3/\text{s}$

longitudinal slope $S = 0.05 \ (20{:}1)$

particle diameter $d_{50} = 0.24 \text{ m}$ (assuming rocks are roughly spherical)

(handwritten: $D = \dfrac{d}{10S} = \dfrac{.24}{10\,(0.05)}$, flow depth $D = 0.48$ m)

The required calculations are shown in Table 2.1:

Table 2.1

EQUATION		UNKNOWN VAR-IABLE	VALUE USED BY WRB	PERCENT DIFFERENCE
$[2.11]$	d = 11DS	D = 0.44 m	D= 0.45 m	2.3
$[2.15]$	n = 0.049d	n = 0.039	n = 0.040	2.6
	L = 6D	L = 4.50m*	L = 3.05	-32.2

*   L = toe protection length.

According to Smith's (1978) criteria, the design proposed by the Water Resources Branch adequately determines the depth of flow and Mannings n, but does not provide sufficient toe protection.

Chapter III

HYDRAULIC MODELS

3.1   INTRODUCTION

Since many hydraulic problems cannot be solved satisfac-
torily by theoretical or empirical methods, hydraulic models
are often an alternative method of determining an economical
solution for a particular problem. Models are particularily
useful where flow conditions are three dimensional, making
theoretical   treatment   difficult.   This   situation often
arises in the design of new hydraulic structures. Because
the flows are generally three dimensional and time depen-
dent,   theoretical analysis is often difficult or impracti-
cal.   At the same time, there may be insufficent experience
with similar structures to enable empirical standards to be
used.

Hydraulic modelling may be considered to be both an art
and a science. The science has evolved sufficiently to per-
mit the development of rules governing model design and an
understanding of the validity of. the solution. Aspects of
the construction,   calibration, and interpretation of the
model results remains largely an art, often relying more on
the experience of the model builder than on his ability to

determine or foresee where model changes should be made in order to make the model and prototype perform more effectively.

Although the design, construction, calibration and operating costs of a model may seem large in isolation, very significant savings can result on the overall project. Because the failure of a hydraulic structure may endanger lives, the savings resulting from a change in design may be more than economic. Obviously, the accuracy of the model results can be very important; a great deal of care must be taken when applying model results to the prototype situation.

The technique of hydraulic modelling is a relatively new branch of hydraulic engineering, dating back about 100 years. One of the major pioneers in the field was Osborne Reynolds, who worked at the University of Manchester and was one of the first to successfully model prototype bed movement patterns. Reynolds' early success involved an element of good luck, since his first choice of sand for the bed material was adequate and his choice of horizontal and vertical scales used a distortion which is considered unacceptable by today's standards. Constructed in 1885, the model of the estuary of the River Mersey used a horizontal scale of 31,800 and a vertical scale of 960 for a scale distortion of 33 (Henderson, 1966). Since the early work of Reynolds and

others, hydraulics laboratories have been set up throughout the world to study basic fluid mechanics phenomena and solve many different types of problems in water resources engineering.

3.2   SIMILITUDE

Three types of similarity are involved in a hydraulic model. For geometric similarity, corresponding lengths in both model and prototype must be proportional. The constant of proportionality is a length scale. For kinematic similarity, times as well as lengths are proportional. This implies that velocities and accelerations will also be proportional. For dynamic similarity, corresponding forces or masses are proportional in addition to the lengths and times.

The conditions for dynamic similarity may therefore be summarized as follows:

[3.1] $\lambda_L = L_p/L_m$; $\lambda_T = T_p/T_m$; $\lambda_F = F_p/F_m$

where λ is a scale, L is a length, T is a time, F is a force, the subscript p refers to a prototype quantity and the subscript m refers to a model quantity.

For most practical hydraulics problems, forces found in the model and prototype may be due principally to pressure (Fp), gravity (Fg), viscosity (Fv), surface tension (Ft),

and elasticity (Fe). In dynamic equilibrium, the inertial force (Fi) balances the vector sum of all the others and this force is given by Newton's second law of motion:

[3.2] $Fi = m*a = \rho*vol*a$

where m is the mass, a is the acceleration, ρ is the mass density and vol is the volume.

The inertial force ratio is therefore:

[3.3] $\lambda_F = \lambda_\rho \lambda_L^3 \lambda_L / \lambda_T^2 = \lambda_\rho \lambda_L^4 / \lambda_T^2$

This equation is known as the Bertrand equation. Each of the five previously mentioned types of forces involved in hydraulic phenomena may be analysed individually, resulting in the following five equations:

[3.4] $\lambda_{Fp} = \lambda_\rho \lambda_L^2$

[3.5] $\lambda_{Fg} = \lambda_\gamma \lambda_L^3$

[3.6] $\lambda_{Fv} = \lambda_\mu \lambda_L^2 / \lambda_T$

[3.7] $\lambda_{Ft} = \lambda_\sigma / \lambda_L$

[3.8] $\lambda_{Fe} = \lambda_E \lambda_L^2$

If pressure force dominates in the system, the other components may be neglected. Therefore,

[3.9] $F_i = F_p$

[3.10] $\lambda_\rho \lambda_L^4 / \lambda_T^2 = \lambda_p \lambda_L^2$

[3.11] $\lambda_\rho \lambda_v^2 / \lambda_p = 1$; $\lambda_v = \text{velocity ratio} = \lambda_L / \lambda_T$

The remaining four forces may be similarly treated if each one by itself dominates the physical process to be modelled.

[3.12] $\lambda_{Fg} = \lambda_{Fi}$; $\lambda_v^2 / (\lambda_g \lambda_L) = 1$ *Froude — gravity*

[3.13] $\lambda_{Fv} = \lambda_{Fi}$; $\lambda_\rho \lambda_v \lambda_L / \lambda_m = 1$ *Reynolds — viscosity*

[3.14] $\lambda_{Ft} = \lambda_{Fi}$; $\lambda_\rho \lambda_v^2 \lambda_L / \lambda_\sigma = 1$ *Weber — surf. tens.*

[3.15] $\lambda_{Fe} = \lambda_{Fi}$; $\lambda_\rho \lambda v^2 / \lambda_E = 1$ *Cauchy — compressibility*

Equations 3.12 - 3.15 are merely ratios of Froude, Reynolds, Weber and Cauchy numbers respectively, accounting for gravity, viscosity, surface tension and compressibility. The pressure ratio may be expressed in terms of the other force ratios as mentioned previously.

In order to obtain true dynamic similarity between model and prototype, all types of forces must be proportional, implying that the Froude, Reynolds, Weber and Cauchy numbers must be the same in both model and prototype. Since the effects of gravity on both the prototype and model are the

same, the gravity ratio is fixed as unity. If the same fluid is used for both prototype and model, the mass and viscosity ratios will also be unity. Because of the limited number of degrees of freedom available, (three for hydrodynamic problems), no one fluid can make all ratios simultaneously equal to unity, so true dynamic similarity is impossible. Fortunately, in many practical situations one effect dominates the other three; by satisfying the dominant ratio requirement and neglecting the remaining ones, valid comparisons are still possible between prototype and model.

In open channel models, gravity effects are always important and quite often dominant, so the Froude number ratio is chosen to be unity. From Equation 3.12, it may be seen that to satisfy this requirement, the velocity scale is the square root of the length scale. Since the velocity scale is the length scale divided by the time scale, the time scale is also the square root of the length scale. Undistorted Froude models use length scales from about 5 to 30 for detailed structures, about 30 to 100 for spillways and about 100 to 1000 for river models.

Compressibility is not significant in open channel flow problems, and surface tension effects can be eliminated by ensuring that the depths and widths of flow in the model exceed 2 cm. A distorted scale model may be necessary to satisfy this requirement. The effects of viscosity may be

quite significant in open channel flow problems, even when
gravity is the dominant force. Since water is generally
used in both prototype and model, the viscosity scale is
unity. The Reynolds numbers in the prototype and model will
therefore be different. Flow in the prototype is virtually
always turbulent (Re > 500). In open channel flow, laminar
flow exists only for Reynolds numbers less than 500. Flows
are fully turbulent for values over 5000. Experience has
shown that scale effects due to viscosity are minimized if
flow in the model is also fully turbulent. Differences in
model and prototype Reynolds numbers are therefore not sig-
nificant as long as both values are in the fully turbulent
range.

BUT NOT IN TRANSITIONAL

The drag coefficients must also be considered if viscosi-
ty effects are to be minimized. If surface drag is insig-
nificant and form drag dominates, the drag coefficients must
be the same in both model and prototype. If surface drag is
significant, the model drag coefficient must be higher than
that of the prototype. This is because the drag coefficient
is highly dependent on the Reynolds number, which is smaller
in the model than in the prototype. The problem is illus-
trated in Figure 3.1. The upper curve shows the situation
dominated by form drag – the drag coefficient is not changed
significantly as the Reynolds number decreases from a high
(prototype) value to a low (model) value. The lower curve
shows the situation dominated by surface drag – as the Rey-

nolds number decreases, the drag coefficient rises substan-
tially.

3.3 UNDISTORTED MODELS

Undistorted models are those in which both the vertical
and horizontal scales are the same. Undistorted models are
used where the flow conditions are of interest at all points
in the model - along edges as well as central portions. For
this reason, structural models are generally undistorted.

Scale ratios for undistorted Froude models are readily
derived from the equation defining the Froude number:

[3.16] $Fr = v/\sqrt{gL}$

Since gravity is the dominant force in an open channel
flow situation, the Froude number in both model and proto-
type must be the same. Squaring both sides of Equation 3.16
and equating model and prototype quantities leads to the
following equation:

[3.17] $v_m^2/(g_m L_m) = v_p^2/(g_p L_p)$

The gravity ratio is unity and so the gravitational con-
stant may be removed from both sides. Velocity is length
per unit of time, giving rise to:

[3.18] $(L_m/T_m)^2 (1/L_p) = (L_p/T_p)^2 (1/L_p)$

[3.19] $L_m/T_m^2 = L_p/T_p^2$

[3.20] $\lambda_T = \sqrt{\lambda_L}$

Mass is the product of density and volume, so

[3.21] $\lambda_m = \lambda_\rho \lambda_L^3$

If water is the fluid used in both model and prototype the mass density scale λ_ρ is unity.

When the scale ratios are known for mass, length and time, any other desired relationships may be determined.

[3.22]
$$\lambda_v = \lambda_L/\lambda_T = \lambda_L^{1/2}$$
$$\lambda_Q = \lambda_L^3/\lambda_T = \lambda_L^{2.5}$$
$$\lambda_F = \lambda_m/\lambda_L = \lambda_\rho \lambda_L^3$$
$$\lambda_p = \lambda_F/\lambda_L^2 = \lambda_\rho \lambda_L$$

3.4 DISTORTED MODELS

Distorted models are used to overcome laboratory space limitations when modelling relatively large areas. The distortion ratio (n) is expressed as the ratio of the horizontal length scale λ_H to the vertical length scale λ_V. For example, a model with a horizontal scale ratio of 30 and a vertical scale ratio of 5 has a distortion of 6. Distortion of the model allows consideration of vertical detail which would be impossible to reproduce in an undistorted model. Distortions usually range from 2 to 7 (Yalin, 1971).

The length in the denominator of the formula for the Froude number (Equation 3.16) is in the vertical direction. A distorted Froude model therefore has a velocity scale equal to the square root of the vertical scale.

Because velocity is defined as the horizontal length per unit of time,

[3.23] $$\lambda_T = \lambda_H/\lambda_v = \lambda_H\lambda_V^{1/2}$$

The discharge scale is therefore:

[3.24] $$\lambda_Q = \lambda_H^2\lambda_V/\lambda_T = \lambda_H\lambda_V^{1.5}$$

Slope of a channel is defined as the vertical change per unit of horizontal change; the slope ratio λ_S for a dis-

torted model therefore becomes λ_V / λ_H and the longitudinal slope in the model is therefore n times steeper than in the prototype. Scale distortion may induce pronounced differences between the model and prototype, particularily at shorelines and other places where the slope of the bed is important. Distorted models are therefore used most sucessfully to model the central portions of channels where depths are relatively large. This type of model is best avoided where three dimensional flow is to be considered.

The greatest advantage of a distorted model lies in its ability to make efficient use of laboratory space and discharge capabilities. Much larger horizontal areas may be modelled without sacrificing vertical detail and the discharge and velocity scales may better suit the laboratory equipment. In addition, distorted models more easily produce fully turbulent flow in river models, allowing rigid modelling requirements to be relaxed.

As an example, consider a channel which may be modelled with either a distorted or undistorted model. The maximum prototype discharge is 100 m^3/ s and the maximum prototype velocity allowable is 2 m/s. If an undistorted model scale (λ_L =50) is used, the model discharge will be 5.6 l/s and the velocity will be 0.283 m/s. If a distorted model is used (λ_H =50, λ_V =10, n=5) the model discharge will be 63.7 l/s and the velocity will be 0.633 m/s. The larger values

of velocity and discharge associated with the distorted model will be more easily measured in the laboratory and will allow better use of the pumps. Since the horizontal scales are the same in both cases, the floor area required for both models is the same.

3.5   FIXED BED MODELS

Fixed bed models may be either distorted or undistorted, and are used when sediment transport is not a concern. A loose granular bed is considered fixed if the maximum flow produces tractive forces below the critical values for sediment transport. In addition, a channel transporting sediment in the vicinity of the bed only (bed load) may be considered to possess a fixed bed if the geometry of the bed does not change significantly through the range of flow conditions under consideration. The bed configuration in this case will be wavelike, with the equivalent roughness determined by the height of the waves.

Form drag is a thrust on an object due to pressure differences between the upstream (high pressure) and downstream (low pressure) faces. Surface drag is the total shear drag over the surface of the object. Because form drag is generally much more significant than surface drag in open channels, the Reynolds number need not be the same in model and prototype if the flows are both fully turbulent. This situ-

ation was previously shown in Figure 3.1. The effect of friction may be considered by examining the Manning equation, which must be satisfied by both model and prototype:

[3.25]
$$v = \frac{1}{n} R^{2/3} S^{1/2}$$

The scale of n is easily determined for an undistorted model:

[3.26]
$$\lambda_n = \lambda_R^{2/3} \lambda_S^{1/2} / \lambda_v$$

The hydraulic radius R has the dimensions of a length.

Equation 3.26 then becomes:

[3.27]
$$\lambda_n = \lambda_L^{2/3} \lambda_L^{1/2} = \lambda_L^{1/6}$$

This equation defines a criterion to model the texture of the bed, namely that the bed should be geometrically similar in both model and prototype. This means that the roughness relative to the depth of flow should also be the same in both cases. As discussed previously, if the flows are fully turbulent, similar Reynolds numbers are not required in the model and prototype. The Reynolds numbers are in fact much lower in the model; consequently, if the roughness is scaled geometrically, the drag coefficient will be higher in the model than in the prototype, since

[3.28] $C_D = (A/2)\rho v^2/F_D$

where F_D is the drag force.   The model therefore will have
proportionately more resistance than the prototype.

Because resistance is very important in river channels, a
distorted model is often used to reduce the exaggeration of
model drag coefficients. Equation 3.26 becomes

[3.29] $\lambda_n = (\lambda_R^{2/3}\lambda_V^{1/2})(\lambda_V/\lambda_H)^{1/2} = \lambda_R^{2/3}/\lambda_H^{1/2}$

The hydraulic radius ratio depends on both horizontal and
vertical lengths.   Although in the prototype the hydraulic
radius is often approximately the average depth,   this may
not be the case in the model.   The ratio may be determined
by calculating the hydraulic radius in each case. The ratio
will be dominated by the vertical scale, ensuring that the
Manning's n will be less than one.   The ratio will only be
one in the case $\lambda_H = \lambda_V = 1$, i.e. a full size model.

In the case of a river model, the scales are generally
chosen so that the model may be made more smooth than the
relationship in Equation 3.29 requires.   In the model cali-
bration process, the roughness may be increased by attaching
small stones or concrete cubes with glue until prototype
conditions are reproduced.   Alternatively, small metal rods
may be attached to the model which extend to the free sur-
face.   Turbulent flow must be produced in the model.   At

least two known prototype flow conditions must be reproduced in the model during calibration tests. More information is needed if the prototype bed and bank roughnesses are different, or if significant berm flow occurs above the main channel.

Structural models, as discussed in the following chapter, are a special type of fixed bed model. Scales are undistorted and surfaces are generally made as smooth as possible, since the effect of roughness is insignificant on the performance of most short spillways.

Chapter IV

EXPERIMENTAL WORK AND TESTING PROCEDURES

4.1   MODEL DESIGN

Two models were used to assess the hydraulic performance
of the proposed drop structures. The structures tested were
based on a design done by the Water Resources Branch with
simplifications made to the geometry as described in the
following section.   Tests to determine the structure rating
curve and discharge coefficients were made on an undistorted
model. A distorted model was built for purposes of compari-
son with the undistorted model and then used to assess
changes in the roughness and permeability of the distorted
structures.

4.1.1   Undistorted Sectional Model

Two models were used to examine the hydraulic perform-
ance of the structures.   A two dimensional model was de-
signed to represent the flow across most of the crest and a
three dimensional model was used to study flow over and near
the sideslopes.   The undistorted model was designed to make
detailed tests on the hydraulic performance of the drop

structures.   In order to make   the study more general,   the geometry of the Water Resources Branch design was simplified by making the   crest width and chute   cross section uniform. In addition,   no excavation below   the existing   stream was considered.   Since   the structure was   to be   considered in isolation, the channel slope and the geometry in the immediate vicinity of the structures   had no significant effect on hydraulic performance.   This permitted the modelling of the structures in a rectangular flume   with a horizontal bottom. In   addition,   the   chute cross   section   was made   constant throughout the length of the structure.   As may be seen in Figure 4.1,   in profile the simplified   structure therefore became a   trapezoidal channel (chute)   through   a relatively wide and   steep slope   (shoulders).   In   cross section   the structure consisted of two sections   as shown in Figure 4.2. The flow   pattern over most of   the crest was assumed   to be two dimensional   while the flow   on and near   the sideslopes was expected to be three dimensional.

In profile,   the two dimensional model   essentially consisted of a triangular rockfill weir with an impermeable cutoff wall   in the crest.   It   was decided to   construct the model in a flume with a width of 0.90 m, a height of 0.75 m, and a length of 13.4 m.   The width of the prototype structure was not   significant since a sectional   model was being considered.   The   prototype crest height   was approximately 2.0 m and the   length was 54 m.   A length   scale of 7.5 was

used for this model. This scale ensured that the model was easily accommodated in the flume. The same length scale was suitable for the three dimensional model, which consisted of the sideslope area along with a short length of the chute floor and a short length of the shoulder on opposite sides as shown in Figure 4.3.

Stones with a d_{50} of 2.3 cm were readily available in the laboratory. The d_{50} of the prototype structures was 24.0 cm. With $\lambda_L = 7.5$, the prototype stone size would be 17.3 cm. If the stones remained stable with $\lambda_L = 7.5$, the stone specification would be conservative, since the stones tested would have only 72% of the diameter and 37.5% of the volume of the stones specified.

The sectional model used had a height of 20 cm and a width of 70 cm. With $\lambda_L = 7.5$ the prototype crest height was therefore 1.5 m.

For the three dimensional model of the sideslope region, a shoulder was added to the two dimensional model and the membrane was extended to follow the crest geometry.

4.1.2 Comprehensive Distorted Model

The distorted model was designed to fit into the same flume as the undistorted model while showing the entire structure. In this case, the flume width was the constraint

which governed the design.   The overall width of the proto-
type structure was 45 m.   Since the model width was limited
to 0.9 m, a horizontal scale of 50 resulted.

Using a vertical scale λ_V = 10 resulted in a distortion
ratio of five. This fell into the acceptable range between
two and seven for such models.   The total prototype struc-
ture height was 2.5 m, so a vertical model scale of ten re-
sulted in a model height of 25 cm.   This height was easily
accommodated in the flume.

For the discharge scale,

$$[4.1] \qquad \lambda_Q = \lambda_H \lambda_V^{1.5} = 50 \ (10)^{1.5} = 1501$$

The prototype design discharge of 24 m^3/s corresponded to a
model discharge of 15.2 1/s.   Model tests to twice the de-
sign discharge were desired; 30.4 1/s was easily accommodat-
ed in the flume.

The dimensions of the distorted model are shown in Figure
4.4.

Since the purpose of drop structures is to dissipate sur-
plus energy, the effect of surface roughness on the hydrau-
lic characteristics of the structure was of interest from
the beginning of the model study.   It was anticipated that
the effects of permeability on this type of rockfill struc-
ture would be significant. It was therefore decided to test

the effects of changes in both roughness and permeability on the hydraulic performance of the structures. Roughness and permeability tests were performed on the distorted model. For these series of tests, the distorted geometry was regarded as a new three-dimensional structure, independent of the previous tests. Distortion was therefore not a consideration in these tests.

Three degrees of surface roughness were considered for the series of tests on roughness (series R). The initial model weir was smooth wood. Two sizes of stones were then attached to increase roughness.

Three degrees of permeability were considered during the series of tests on permeability. The initial wood weir was made impermeable by sealing all joints with silicone. A single layer of stones was then attached to the wood, making only the top layer of the structure permeable. Finally, a completely permeable weir of the same geometry was constructed.

4.2   MODEL CONSTRUCTION

4.2.1   Undistorted Model

A trial run prior to construction of the undistorted models indicated that uncontrolled tailwater levels would create a high degree of submergence of the structure at high discharges due to the flat slope of the flume. In order to

obtain the most severe conditions for stone stability, the greatest practical difference between headwater and tailwater levels was desired. A low tailwater level was maintained by placing the model on a platform in the flume which raised the entire structure 15 cm, as shown in Figure 4.5. This platform lowered tailwater elevations substantially at all discharges.

When the two prototype structures were observed in August, 1981, it was noted that a pool of water was held above the upstream structure despite a very low discharge. Fine shale and silt had filled the void spaces in the rockfill, rendering it relatively impermeable. To duplicate this condition in the model, silicone was placed in all joints upstream of the membrane. This ensured that all water going through the flume passed over the membrane of the weir, eliminating throughflow across the crest cross section.

A silica sand bed was placed downstream of the model to provide an erodible bed. The d_{50} of the sand used was 0.21 mm. Tailwater levels were controlled with a vertical lift tailgate installed in the downstream end of the flume. Because of the amount of sand lost during preliminary tests, a wooden sill was added to trap sand in the downstream end of the flume. A V notch weir was installed at the upstream end of the flume to measure small discharges.

4.2.2 Distorted Model

The distorted model was constructed of 1 cm plywood and installed in the flume as a unit, mounted on boards 3.8 cm thick. This slight raising of the weir had a negligible effect on the weir height but permitted the addition of a layer of stones in the vicinity of the structure and also reduced tailwater levels slightly. The wooden form was made impermeable by sealing all joints with silicone. The sideslopes upstream of the crest were difficult to fit with wood; tin was substituted to obtain a smooth transition.

When testing with the smooth wood weir was complete, the first grade of stones was glued to the surface of the structure. Because the stones were relatively small, (d_{50} = 8.5 mm), contact cement was applied to the wood and the stones were poured over the surface and pressed into the glue. On the upstream slope the stones were placed individually near the crest, and the lower areas were permitted to remain nearly smooth.

After testing had been completed with a roughened weir, the larger stones were glued onto the smaller stones. The median diameter of the larger stones was 23 mm. Pouring these stones into a layer of contact cement was ineffective; the stones were eventually all dipped into the cement and placed individually. This procedure was relatively expensive and time-consuming, but the final surface proved very durable.

4.3   MODEL TESTING

Similar tests were run on both distorted and undistorted models.   Upstream water levels were recorded for both models so that the rating curves could be developed.   Tailwater levels were also measured to ensure that the weirs were not affected by submergence.   Water levels along the structures were recorded for some tests.   Tests were started at a low discharge, usually in the range of 4-6 l/s.   For the undistorted models, the tailwater levels were raised as quickly as possible by starting with the tailgate closed.   Erosion on the silica sand bed was therefore minimized.   Testing started after all air pockets in the model and its supporting platform were filled with water and the downstream silica sand bed was saturated.   Similar procedures were used for the distorted model, except that no precautions were necessary to prevent erosion of the downstream bed, since the distorted model used a fixed bed.   The discharge was set near the desired amount using the upstream V notch weir for flows less than 30 l/s and a venturi meter in the water supply line for discharges over 30 l/s.

The water supply line entered the flume through two valves which were operated to make the flow at the inlet of the flume as uniform as possible.   The water then flowed through a baffle consisting of short pipe sections stacked parallel to the flow.   Another baffle consisting of two

steel grates was installed downstream of the V notch weir. The water then flowed through the testing section of the flume and discharged into one of two volumetric discharge tanks. After passing through these tanks, the water re-entered the laboratory sump. The water was recirculated by centrifugal pumps with capacities up to 65 l/s. Excess water was discharged through relief valves and returned directly to the sump. The capacity of the system was limited by the flow capacity of the flume with the V notch weir installed. The 65 l/s discharge eliminated freeboard at the inlet end of the flume. Figure 4.6 shows a schematic representation of the laboratory facilities used.

After the discharge had been run for 10-15 minutes to allow time for flow stabilization, all point gauges were read and the discharge was measured with a volumetric tank. Point gauges were located in piezometric wells outside the flume connected by siphons to the headwater and tailwater pools. In addition, a point gauge mounted on a travelling carriage was used to determine water surface profiles and to check head and tailwater elevations. This gauge was also used to set and check all bed and weir elevations. All gauges and the discharge were again checked after 5-10 minutes to ensure flow stability. If readings had changed more than 1 mm, the system was allowed to run until two consecutive sets of readings were within the 1 mm limit. Because of the relatively small size of the system, stability was

generally achieved quickly and could be maintained for long periods of time.

This procedure was repeated with increasing discharges until a desired limit was reached or a structural failure took place. The upper discharge limit varied from model to model; some tests were continued until the discharge capacity of the flume was reached. Photographs were taken after many runs, particularly those near the design discharges and maximum discharges. Following a failure or significant movement of stones in the chute of the undistorted model, the bed profile was checked with the moveable point gauge. To preserve patterns created by the flow conditions, each series of tests ended by closing the tailgate to bring the tailwater levels up. The flume was then allowed to drain slowly over several hours.

Plates 7 and 8 show the undistorted two dimensional model before and after testing. Plate 9 shows the undistorted three dimensional model before testing. Plate 10 shows the same model at the maximum discharge tested and Plate 11 shows the model following this test. Plates 12 - 18 show the models used to assess the effects of roughness and permeability. Plate 12 shows the smooth impermeable wood model while the top layer permeable models roughened with stones having representative diameters (d_{50}) of 8.5 mm and 23 mm respectively are shown in Plates 13 and 14. In each

of these tests the model is shown operating at the design discharge. Plates 15 and 16 show the roughened top layer permeable model (d_{50} = 23 mm) operating at the maximum discharge tested. Plates 17 and 18 show the completely permeable model (d_{50} = 23 mm) operating at the design discharge.

4.4 WATER SURFACE PROFILE MODEL

Physical models were used during the study to investigate the hydraulic characteristics of the structures in isolation. The results gave no indication of the effect of the structures on flow characteristics in the channel. In order to study the impact of the structures on water surface profiles and velocities, a mathematical model was used. The HEC-2 Water Surface Profile program was run for three conditions - the idealized channel before the installation of a structure, the same channel immediately after the construction of two weirs, and the same channel after the pools upstream of the weirs were filled with sediment.

The simplified channel used throughout the tests consisted of a single cross section repeated along the entire channel length. This cross section was derived by overlaying 33 surveyed cross sections which were provided by the Water Resources Branch, and averaging by eye. Bends were not considered in the simplified problem. In contrast, the natural stream channel was irregular and contained many bends. As

shown in Figure 1.2, some of the prototype structures were located on bends and all were in close proximity to bends. In addition, the natural channel was braided, with the thalweg crossing back and forth across the canyon.

The HEC-2 program was developed by the US Army Corps of Engineers Hydrologic Engineering Center. The first version was developed in 1964; the version used was issued in November 1976. The program is 9,400 lines long; a description of the entire program is not available. The users manual (Hydrologic Engineering Center, 1976) provides an excellent description of the many options available for the program as well as the input requirements. A brief description of the input data and important options is presented here.

Input to the program consists of a discharge at a reference cross section where flow parameters and channel characteristics are known. An estimate of the energy slope and water surface elevation or a known water surface elevation at the reference cross section and the Mannings n of the channel is also required. All channel geometry is referenced from the previous cross section.

Multiple profiles may be run for the same geometry by including a table of discharges to be used. This option is highly recommended, since the program will then only be compiled once. This results in very substantial savings in computer time. Another option permits the Mannings n to be

varied horizontally and vertically. The discharge may be increased or decreased at a cross section to model branches or confluences. Imperial or metric units are chosen for the entire program with the specification of a single option. Many options are available to control output. If the number of cross sections used exceeds five, a profile is printed automatically. Any or all input cross sections may be plotted to show the water surface.

For each of the three series of tests run with the model, six discharges were used. In addition to the 24 m^3/s design discharge, discharges of 6, 12, 18, 36, and 48 m^3/s were used, giving a testing range from 25% to 200% of the design discharge. The first series of tests used the simplified channel without any structures. This series represented conditions before construction of the weirs. The second series used the same channel with two idealized weirs representing the conditions immediately following construction of the weirs. The third series of tests used the same channel and weirs with the upstream pools filled to the level of the crests. The bed therefore extended horizontally upstream from the weir crests to a point where the normal bed slope re-emerged. This geometry represented conditions with the pools filled with sediment.

Water surface profiles were obtained for each of the six discharges in each series of tests. Additional data was ob-

tained at each cross section for each discharge and geometry. This additional data included average velocities, cross sectional areas and energy slopes.

4.5   ANALYSIS OF TEST RESULTS

This section describes general aspects of the analysis of the results obtained with all models, both physical and mathematical. This material is intended to serve as an introduction to the detailed analysis and discussion of results which follows in Chapter V.

4.5.1   Physical Model Tests

The development of a rating curve for the idealized prototype structure was a primary purpose of the physical modelling program. To obtain the rating curve, information from both the two dimensional and the three dimensional undistorted models was combined. Since the same length scales were used, the models had the same crest height and longitudinal slope and were made of the same material. Combination of the results was therefore a relatively straightforward process. An example of the technique used is shown in Figure 4.7.

For any particular head, the first step consisted of determining what portion of the entire structure was represented by the three dimensional model. The remaining crest

width from the center line to the portion represented by the three dimensional model was multiplied by the unit discharge (q) corresponding to the same head from the two dimensional model. For very high discharges the shoulders were overtopped. The shoulder region had the same geometry as the sectional model except that the elevation of the "crest" was raised by the height of the chute. That portion of the shoulder width which was not included in the three dimensional model was therefore again multiplied by the unit discharge for the corresponding head from the two dimensional model.

In this way, the total discharge for one side of the model could be determined by adding the discharges for each of the three areas – the sideslope area represented by the three dimensional model and the sectional chute and shoulder areas represented by the same two dimensional model, since the drop structure was symmetrical. The final step of the procedure consisted of doubling the resultant discharge to account for the second half of the model.

A rating curve was later developed in the same way for a second pair of models with a 15:1 longitudinal slope.

Once rating curves were available for the models and their equivalent prototypes, several comparisons were possible. The comparison between the 20:1 and 15:1 longitudinal slopes was of great practical interest, since the longitudi-

nal slope affects the volume of the prototype structure and hence its cost.

The combination rating curve discussed to now was developed for a chute with a trapezoidal cross-section. The sectional model alone was used to determine the rating curve for two additional chute geometries which were then compared to the trapezoidal geometry. The equivalent rectangular chute had the same height and cross-sectional area as the trapezoidal chute. A small rectangular chute which had the same width as the bottom of the trapezoidal chute was also considered. The difference between the trapezoidal chute and small rectangular chute was the cross-sectional areas over the sideslopes. The sum of these triangular areas was then compared to an equivalent triangular weir. The purpose of these comparisons was to determine whether or not a simple theoretical method could be found to approximate the performance of the model structure's rating curve.

In profile, the central chute section of the weir was triangular. The sectional model results were therefore compared to a theoretical triangular profile, as well as sharp crested and broad crested profiles.

The effects of changes in chute depth, weir height, and roughness were investigated by changing the length scale from 7.5 to 10. These comparisons were made in terms of unit discharges based on the results of the two dimensional (undistorted) model.

Since the same structure had been modelled with both distorted and undistorted models it was possible to compare the effect of scale distortion. Data from the distorted model also allowed comparisons of three degrees of roughness and permeability.

For each of these comparisons, the effect of the geometry change on the rating curve of the structure was obtained.

4.5.2   Mathematical Model Tests

The HEC-2 backwater profiles model was used to assess the effect of the structures on the entire reach of the stream. In the first test, the original channel rating curve was determined by using six discharges in the idealized channel without structures. The discharges used ranged from 6 m3/s to 48 m ^{3}/s; the design discharge was 24 m^3/s. The channel geometry used in the test is shown in Figure 4.8. The second test determined water surface profiles for the same discharges with two idealized weirs installed. The channel used is shown in Figure 4.9. In the third test, the same discharges were used with a modified channel. The bed was extended horizontally upstream from the crest of each weir to the point where the natural slope intersected the flat bed. This situation represented conditions with the upstream pools filled with sediment and is shown in Figure 4.10.

Two structures were sufficient to model the entire reach because the conditions between each set of weirs were assumed to be the same for the idealized problem considered. The channel cross section was constant throughout the reach and all structures were identical. Since the bed slope was constant, the spacing required between pairs of structures was also the same. Only two weirs and the appropriate length of channel separating them were therefore required in the mathematical model; additional length would have been repetitive.

In each test, the water surface profile was of interest for the purpose of comparisons between tests. In addition, the profiles showed immediately that the weirs were not significantly submerged by the pools created by the downstream weirs. Submergence to greater than 80% of the height of the structures would have affected discharge conditions at the crests so that conditions downstream of the weirs would have exerted some control over conditions upstream of the weirs.

Comparisons between water surface profiles for the same discharge indicated the effects of the structures on flow conditions in the channel with and without the structures installed and with and without the upstream pools filled with sediment.

Average cross sectional velocities and flow areas were calculated by the model for each input cross section. These

values, although not used in this study, would be of value in assessing erosion and sediment transport under the conditions tested.

A detailed discussion of the results obtained with all models follows in Chapter V.

Chapter V

RESULTS AND DISCUSSION

5.1   PROTOTYPE RATING CURVE

Model and prototype rating curves were developed using the technique described in Section 4.5.1. The prototype rating curve for the structure with the 20:1 longitudinal slope is shown in Figure 5.1. This curve is well supported by experimental results up to the shoulder elevation; only one point was obtained above this height. A sharp break occurs in the rating curve at the shoulder elevation, reflecting the greatly increased crest length available when over shoulder flow occurs. The head required to pass the 24 m^3/s design discharge is 0.728 m. The design discharge is therefore confined to the trapezoidal chute.

In the design proposed by the Water Resources Branch, a normal depth of 0.45 m was determined in the chute, assuming a Manning's n of 0.046. The critical depth of the design discharge is 0.526 m. The steep longitudinal slope (5%) ensures flow in the chute will be supercritical for values of n below 0.060. The assumed value of n=0.046 therefore appears to be reasonable and the 0.30 m freeboard allowance in the chute is adequate. As a matter of interest, flow at the

design discharge will be contained within the chute if n < 0.11, although the flow will no longer be supercritical. Little freeboard (0.02 m) is available on the upstream side of the crest at the design discharge. Although drawdown near the chute would increase this value, overtopping of the crest would be possible at the sides of the channel at the design discharge.

5.2 PROTOTYPE STABILITY AND FAILURE MODE

As discussed in Section 4.1.1, the volume of the stones used in the models was only 37.4% of the volume required for geometric similarity. Despite the relatively small stone size used for the model, all structures tested remained stable at discharges considerably above the design discharge. As the discharge was increased, prominent stones on the chute floor vibrated until they gained a more stable position or were dislodged and rolled downstream. A very small portion of the bed exhibited this behavior.

Failure occurs in the three dimensional model with the 20:1 longitudinal slope at a head of 11.49 cm, corresponding to a head of 0.862 m on the prototype. Estimation of the discharge at this head requires extrapolation of the rating curve shown in Figure 5.1. The corresponding prototype discharge would be in excess of 40 m^3/s and most likely near 48 m^3/s, or twice the design discharge.

The method of failure is illustrated in Figure 5.2. The toe was first lowered by the removal of both stone and sand at the downstream transition between the structure and the sand bed. This caused steepening of the 4:1 sideslope near the toe, leading to flow concentration at the bottom of the chute. Flow concentration in turn removed more material at the toe, completing the cycle of events leading to failure.

When sufficient material had been removed from the bottom of the structure, a sudden progressive slope failure occured along the chute floor. This failure initially extended vertically to the solid floor under the model. The failure quickly extended upstream until the depth of stone prevented exposure of the solid floor. Antidunes were formed on the reworked chute floor downstream of the failure.

The method of failure was similar to that described by Smith (1978). Smith's failure mode also involved an upstream progressive failure of the longitudinal slope. The principal difference between the two modes was the point at which the failure stopped. Smith's structure used a uniform stone thickness along most of the longitudinal length, with greater depths of stone occurring only in the vicinity of the crest. The failure therefore was not halted until the crest area was reached. In the design tested in the present study, the triangular profile provided a sufficient depth of stone to halt the failure well short of the crest.

5.3   EFFECTS OF GEOMETRY CHANGES

Several changes in geometry were investigated during the course of physical model testing. In addition to these changes, several theoretical rating curves from common weir shapes were compared to the observed rating curves developed during testing.

5.3.1   Effect of Downstream Slope and Weir Profile

Two downstream slopes were tested in the physical modelling program. The standard 20:1 slope was tested initially and later a 15:1 slope was tested. Rating curves for the entire structure were developed for each slope as explained in Section 4.5.1. These curves are shown in Figure 5.3. The performance of the structure with the 15:1 slope is very similar to that with the 20:1 slope. At the design discharge, the head on the 15:1 structure is 0.724 m. The difference between this head and the corresponding head on the 20:1 structure is 0.004 m or 0.55%. The prototype performance of the structure with the steeper longitudinal slope therefore would be virtually identical to that of the standard structure, although some reduction in construction costs would result from the smaller volume of rockfill required. Alternatively, rock saved by the construction of the smaller structure could be used for bed and bank protection immediately downstream of the toe of the structure.

A comparison of the unit discharge rating curves from the standard 20:1 longitudinal slope model and theoretical broad crested and sharp crested weirs is shown in Figure 5.4. The comparison was made in order to determine whether or not characteristics of the structure to be tested could be predicted from easily derived theoretical rating curves. Since the geometry of the triangular profile tested lay between that of a broad crested and sharp crested weir, it was reasoned that either of these well known profiles could be used to approximate the triangular structure for preliminary design purposes. As may be seen in Figure 5.4, the sharp crested profile provided the better approximation for higher unit discharges ($q > 0.7 q_d$ where q_d is the design unit discharge). For $q < 0.7 q_d$, the model rating curve fell almost exactly halfway between the theoretical rating curves. At the design unit discharge, the head predicted by the sharp crested weir was 0.15 cm or 1.5% less than that measured on the model. At the same discharge, the broad crested weir overestimated the head required by 0.6 cm or 6.1%.

5.3.2 Effect of Chute Cross Section

Three chute cross sections were investigated with the physical models. The purpose of the investigation was again to determine whether or not the hydraulic performance of the structure could be predicted by a similar model with a more simple geometry. In addition to the studied trapezoidal

chute cross section, two rectangular chutes therefore were considered. The equivalent rectangular chute had the same depth and cross sectional area as the trapezoidal chute. The reduced rectangular chute had the same depth and bottom width as the trapezoidal chute. The difference in cross sectional area between the trapezoidal and reduced rectangular chutes therefore was the area over the sideslopes on the trapezoidal chute. Since the addition of these two areas produced a triangular chute, the possibility of representing this area with a V notch weir was also investigated.

The trapezoidal chute rating curve was developed from the combination model tests for the 20:1 longitudinal slope as previously discussed. The rating curves for the two rectangular chutes were developed from the two dimensional model alone. All three rating curves are shown in Figure 5.5, along with a diagram comparing the cross sections used for each rating curve. The equivalent rectangular chute provided a good approximation for the trapezoidal chute, varying by 0.13 cm or 1.5% at the design model discharge. This accuracy is sufficient for preliminary design purposes. The reduced rectangular cross section rating curve did not accurately predict the rating curve of the trapezoidal chute model. The reason for the poor approximation was the longer effective crest length provided by the sideslope areas.

In view of the foregoing discussion, flow passing over the shoulders of the trapezoidal model was clearly significant. In order to determine whether or not this flow could be approximated with a V notch weir, the rating curve for the over shoulder flow was plotted with the rating curve for a V notch weir as shown in Figure 5.6. The theoretical curve was developed from analyses presented by Smith (1978), and Brater and King (1976). The probable reason for the discrepancy between curves is that the theoretical curves are based on thin plate V notch weirs, while the model curve is influenced by friction and geometry similar to that of a broad crested weir.

A theoretical equation has been developed by Smith (1978) specifically for a trapezoidal crested weir. This equation includes terms for both flow regions considered in the present study. The equation of the rating curve is as follows:

[5.1] $$Q = 1.70 \, BH^{1.5} + 1.27 \, \tan(\theta/2)H^{2.5}$$

The first term is the equation for a broad crested weir and accounts for flow over the rectangular portion of the crest. The second term is an equation for a V notch weir with an angle of θ. This term accounts for flow over the sides of the crest. A comparison of this rating curve and the one developed by model tests is shown in Figure 5.7. Two reasons are apparent for the divergence of theoretical

and model curves at higher discharges. As already dis-
cussed, the performance of the rectangular portion of the
chute is better represented with a sharp crested weir rather
than a broad crested weir. In addition, the V notch equa-
tion is not an ideal approximation of the over shoulder por-
tion of the flow. Since both portions of the model pass
discharges at lower heads than the theoretical curves pre-
dict, the combined model discharge requires considerably
less head than the combined theoretical curve predicts.

For design purposes, the best approximation to flow in
the trapezoidal chute therefore appears to be that given by
the equivalent rectangular weir. The performance of this
weir could in turn be predicted by a sharp crested weir of
the same width. The steps in predicting the rating curve
for a trapezoidal chute would be as follows:

1. Determine area of trapezoidal chute and divide by
   chute height to obtain width of equivalent rectangu-
   lar weir.

2. Determine rating curve for a sharp crested weir of
   the width calculated in Step 1.

A prototype rating curve using this procedure is compared
to the rating curve developed from model tests in Figure
5.8.

5.3.3   Effect of Scale

The effect of scale on the prototype rating curve was studied with the two dimensional model with the 20:1 longitudinal slope.   A change in length scale from 7.5 to 10 resulted in a prototype structure with a higher crest and a longer profile, although the slopes of the profile remained the same.   The size of the roughness elements also increased.   The rating curves resulting from each scale are shown in Figure 5.9.   Although the hydraulic performance of the structures is similar throughout most of the testing range, it may be seen that the lower weir (λ_L = 7.5) passes more discharge at a given head.   The reason for the difference in curves lies in the scale ratios used in the axes of the graph.   The ratio of length scales is 7.5/10 or 0.75. This ratio relates all head measurements for the vertical axis.   The unit discharge ratio is not the same, since the scale used is $\lambda_q = \lambda_L^{1.5}$.   This makes the ratio between the curves 20.54/31.62 or 0.65.   Since the original model values are being multiplied by different ratios, the prototype curves diverge.

5.3.4   Effect of Scale Distortion

Structural models are normally built without distortion so that three dimensional flow patterns may be maintained. Little information is available on the consequences of dis-

torting the scale ratio. To test the effect of such a distortion on the structure under consideration in this study, a model was built with a horizontal scale of 50 and a vertical scale of 10. The dimensions of the model are shown in Figure 4.4. The model was not identical to the undistorted model, since an impermeable wooden shell was used under the stones rather than a single cutoff at the crest. The shell was covered with one layer of stones which was glued to the wood, making slope failure impossible. The effect of permeability below the top layer therefore was assumed to be insignificant. According to Olivier (1967), most flow in rockfill structures occurs in the top layer of stones.

The stones used for both distorted and undistorted models were the same size (d_{50} = 23 mm). To obtain the same chute depth with both models, a length scale of λ_L = 7.5 was required for the undistorted model. The roughness was therefore not scaled geometrically, since the vertical scales used in the models were different.

Rating curves for the prototypes corresponding to both models are shown in Figure 5.10. The curves are very similar and both predict nearly the same head required to pass the design discharge of 24 m^3/s. Unfortunately, the similarity between the curves is largely due to distortions in the model roughness which were caused in part by the selection of different vertical scales in the models.

Roughness may be scaled on the basis of Mannings n or grain size (Sharp, 1981). Manipulation of the Mannings formula yields:

[5.2] $$n_p/n_m = (L_p/L_m)^{1/6}$$

Grain size is scaled geometrically with the length ratio:

[5.3] $$k_p/k_m = L_p/L_m$$

The undistorted model used a length scale of 7.5, leading to an n scale of $7.5^{1/6}$ or 1.40. For the distorted model, a vertical length scale of 10 led to an n scale of $10^{1/6} = 1.47$. (The vertical scale dominates roughness effects in a distorted model). The two models therefore used n scales which differed by approximately 5%. Basing the roughness on the grain size criterion of Equation 5.3 leads to grain size ratios of 7.5 and 10 for the undistorted and distorted models respectively. The grain size ratio therefore varied between the models by 33%.

5.3.5 Effect of Roughness

The effects of roughness were investigated with the distorted model, which for this purpose could be considered an entirely different prototype structure, since this series of tests was not connected to previously discussed results.

Dimensions of the model are shown in Figure 4.4. Three degrees of roughness were considered - smooth wood, and a wood surface roughened with stones having a d_{50} of 8.5 mm and stones having a d_{50} of 23 mm. Problems were experienced in determining the correct datum for this series of tests, since some water flowed through the layer of stones glued to the crest. The datum for all three curves was finally chosen to be the top of the wood crest. This choice was based on the assumption that the amount of water flowing through the stones was a more important consideration than the amount of cross sectional area occupied by the stones. The rating curves shown in Figure 5.11 indicate that this assumption was poor, since the curves differ by approximately the thickness of the stone layers. This result indicates that the amount of flow through the stone layer at the crest is very small relative to the amount flowing over the stones. This will be discussed further in the following section.

Water surface elevations at several points along the chute were measured at various discharges for all three degrees of roughness. The most consistent results were obtained through the chute centerline, where the elevation was measured at the crest and at stations located 30 cm and 55 cm downstream. Nominal velocities at the cross sections were calculated from the depths and the energy grade lines were determined. The overall energy loss per unit of chute

length on the smooth weir was 0.05 cm/cm, although the loss
was not consistent along the length. The 8.5 mm stones pro-
duced a consistent loss of 0.20 cm/cm and the 23 mm stones
produced a reasonably consistent loss of 0.25 cm/cm. The
energy loss therefore increased with roughness, but in a non
linear manner. Insufficient data was available to determine
a quantitative relationship between roughness and energy
loss. The results obtained suggested that a longer slope
with more cross sections would be required to better define
this relationship.

5.3.6   Effect of Permeability

Permeability effects were investigated with the distorted
model, again assuming that the distorted geometry could be
considered as an undistorted model of a different structure.
Changes made to the structure to alter roughness also al-
tered permeability, making the separation of these effects
difficult. The smooth wood model was completely imperme-
able, while both stone covered models were permeable in the
top layer only. In order to test a third change without in-
volving changes to roughness, a completely permeable struc-
ture was built with the 23 mm stones to the same dimensions
as the other weirs. Comparisons are therefore possible be-
tween the completely impermeable and top layer permeable
weirs and the completely permeable structure. Rating curves
for all three structures are shown in Figure 5.12. The

curves for the impermeable and top layer permeable weirs are the same as are shown in Figure 5.11, except that the datum for the top layer permeable structure has been raised by 23 mm to the top of the stone layer. This was done to make the datums comparable for the top layer permeable and completely permeable weirs.

Although roughness is a factor in the rating curves for the impermeable and top layer permeable structures, it may be seen that little flow occurs in the single stone layer at the crest. Olivier (1967) indicates that a large portion of throughflow takes place in the upper rockfill layers. While this is true at low discharges, the conditions tested in this study used discharges high enough to ensure that overflow was much larger than throughflow. Flow through the top layer of stones therefore became insignificant. The completely permeable structure passed 7 1/s as throughflow without overtopping the crest and failed at a discharge of 22.6 1/s. The failure occurred suddenly after conditions appeared to have stabilized. When throughflow takes place, failure is encouraged by outward flow on the downstream face as well as the tractive force of the overflowing water.

In order to quantify the effects of permeability, further tests would be required to separate the effects of roughness and permeability.

5.4   INITIAL BACKWATER EFFECTS

Three series of tests were carried out with the HEC-2 backwater model. The first series used a straight channel without structures - the initial condition. Discharges of 6, 12, 18, 24, 36, and 48 m³/s were used. The same discharges were then used in an identical channel with two structures inserted. The geometry of the structures was identical to that tested in the physical model tests. This series modelled conditions immediately after the installation of the structures. The final series used the same discharges and weir geometries, but was modified by the assumption that all storage space upstream of the crest was filled with shale. This series approximated conditions after sedimentation had occured upstream of the structures.

5.4.1   Series A - Initial Conditions

Series A involved a steady flow in a uniform channel, as shown in Figure 4.8. As might be expected, identical velocities, depths, and areas of flow were calculated at each of the seven cross sections used, indicating normal flow conditions were occurring for each of the six discharges used. The model therefore effectively determined the channel rating curve. This rating curve is shown in Figure 5.13. The simple conditions tested in Series A were a trivial test of the powers of the HEC-2 model. However, in addition to de-

veloping the initial channel rating curve, the series provided a shakedown run of the model prior to the testing of the more complex geometries in the following series.

5.4.2 Series B - Conditions Immediately Following Construction

Series B introduced the rockfill structures into the channel tested in Series A. The structures were implicitly assumed to be impermeable and a uniform roughness was assumed for the structures and channel (n = 0.04). The geometry of the channel and structures is shown in Figure 4.9. The use of twelve cross sections permitted the modelling of two complete structures as well as upstream and downstream sections. A rating curve was developed at cross section 6, which was located 4.9 m upstream of the crest of one of the structures and away from the drawdown zone as shown in Figure 4.9. This rating curve is shown in Figure 5.14. For comparison, the rating curve developed by the physical model tests is also shown. The similarity between the curves is good until the shoulder elevation is reached. The physical model results consistently predict slightly better hydraulic performance than the HEC-2 model. At the design discharge of 24 m^3/s, the difference in heads predicted by the two models is 0.05 m or 7%.

Maximum velocities in the channel system occurred in the chutes of the structures. At the design discharge, a maxi-

mum velocity of 2.20 m/s was calculated at the crest of the structures. Channel velocities downstream of the structures generally remained below 2.0 m/s at all discharges. Velocities through the pools were reduced to below 0.5 m/s immediately downstream of the structures for most discharges. The only exceptions occurred at discharges above the design discharge.

A profile of the water surface at the design discharge of 24 m^3/s is shown in Figure 5.15.

5.5   WATER SURFACE PROFILE WITHOUT POOLS

Series C in the HEC-2 series of tests used the channel and weir geometry of Series B with the pools filled level to the crests of the structures with sediment. The geometry involved is shown in Figure 4.10. Sixteen cross sections were used.

A rating curve for the structures was developed at cross section 5, which was the nearest section upstream of the crest. Although the section was only 2.25 m from the crest and therefore in the probable drawdown zone, experience with Series B indicated that the HEC-2 model was not sensitive to drawdown. In Series B, little difference was observed in flow characteristics at distances of 4.9 m and 2.8 m from the crest. The rating curve from Series C is shown in Figure 5.16 along with the rating curve from Series B for the

purposes of comparison. The curves correspond closely at all discharges, indicating that the loss of the pools to sedimentation has little effect on the hydraulic performance of the structures. Since velocities in the chutes were supercritical, depths and velocities of flow produced in the chutes were identical at all discharges in Series B and C. Channel velocities between the structures and the downstream pools were also unchanged in both series. Velocities over the pools in Series C increased due to the reduced cross sectional area. Velocities were reasonably constant at approximately 1 m/s over the channel sections where sedimentation had been assumed. The water surface profile generated by the design discharge in Series C is shown in Figure 5.17.

5.6   APPLICABILITY OF STRUCTURES

All physical and mathematical model testing done in this study involved structures in a straight uniform channel. It is therefore impossible to predict in detail how the prototype structures on Wilson Creek will perform, since these structures are located near and even in bends of the streambed. Results of the study indicate that the structures tested would function as effective gradient control structures in straight uniform channels such as irrigation canals or drains. The weirs are able to substantially reduce velocities where pools are formed and continue to function (although less efficiently) after the pools are filled with

sediment.   The loss of the pools upstream of the structures
has little effect on the hydraulic performance of the weirs
themselves.   For maximum effectiveness, the heights of the
structures in a series should be chosen so that the backwa-
ter effect from one structure extends to the toe of the next
upstream structure, thus reducing velocities along the en-
tire channel.   Results of the HEC-2 series of tests indicat-
ed that channel velocities of 1.0 - 2.0 m/s remained in
reaches which were unaffected by backwater.   These veloci-
ties would be erosive on streambeds such as Wilson Creek,
since erosion has occurred on Wilson Creek at a mean channel
velocity of 1.5 m/s (design conditions).

Sedimentation problems on Wilson Creek are largely the
result of bank erosion in a meandering channel caused by si-
decutting at the bends.   The structures tested in this study
are useful for bed protection only, and will provide very
little bank protection.   Although flow depths will increase
and nominal velocities will decrease as a result of the
structures, the current at the bends, although reduced, will
continue to erode the outer banks regardless of the depths
of flow.   The Wilson Creek gradient control structures can
therefore not be expected to have a significant long term
effect on erosion and sedimentation patterns.   A reduction
in downstream sedimentation may be anticipated while the
pools fill with sediment and the streambed seeks to regain
its natural slope.   Given the relatively small volume of

sediment storage provided by the pools and the extreme range of water and sediment discharges observed in this type of stream, the duration of the possible improvement will be short. Periodic removal of the sediment from the pools would maintain the effectiveness of the structures as sediment traps.

Chapter VI

CONCLUSIONS

1. The physical model tests indicated that the rockfill structures tested will remain stable well beyond the design discharge. When failure occurs, the failure mode is progressive, starting at the toe of the structure and proceeding upstream until the depth of stone is sufficient to prevent removal.

2. The hydraulic performances of the model structures with 20:1 and 15:1 downstream longitudinal slopes are not significantly different in the range of discharges tested. Further investigation would be of value to determine a minimum acceptable slope for such structures.

3. The rating curve for the tested trapezoidal chute can be approximated with sufficient accuracy for preliminary design purposes by a sharp crested weir having the following equation:

$$[6.1] \quad Q = 2.95 \ B \ \left[0.611 + 0.08 \frac{H}{W} \right] H^{3/2}$$

where B is the crest length

H is the head on the weir

W is the weir height

The crest width B may be determined by the following equation:

[6.2] $B = b + D \times SS$

where b is the bottom width of the chute

D is the depth of the chute

SS is the sideslope of the chute

Further testing is required to confirm this approximation for other geometries.

4. Further testing is necessary to separate and quantify the effects of roughness and permeability on rockfill drop structures.

5. The HEC-2 model indicated that the structures tested could reduce average channel velocities in the pools above the weirs from approximately 1.5 m/s to between 0.5 and 1.0 m/s at the design discharge of 24 m^3/s . The structure rating curves given by the physical and mathematical models agree well over the range of discharges up to and including the design discharge.

6. The filling of the pools above the tested weirs with sediment does not significantly affect the rating curves of the structures. Velocities are reduced to approximately 1.0 m/s over the filled pools, but remain at erosive levels (1.0 - 2.0 m/s) in reaches not affected by the pools.

7. The structures tested would be effective for gradient
   control (bed protection) in straight uniform chan-
   nels. They cannot be expected to eliminate bank ero-
   sion in meandering streams.

REFERENCES

Allen, J. Scale Models in Hydraulic Engineering. London:
    Longmans Green and Co., 1947.

Blais, E.-L. and McGinn, R. A. "An Investigation of Critical
    Erosion Velocity for Natural Shale Gravels." Albertan
    Geographer, No. 15, 1979.

Blench, T. "Scale Relations among Sand Bed Rivers including
    Models." Proceedings Separate No. 667, ASCE, Vol 81,
    1955.

Brater, E.F., and King, H.W. Handbook of Hydraulics for the
    Solution of Hydraulic Engineering Problems, Sixth
    Edition. New York: McGraw-Hill Book Company, 1976.

Carlyle, W.J. "The Management of Environmental Problems on
    the Manitoba Escarpment." Canadian Geographer, Vol 24,
    No. 1, 1980.

Einstein, H.A., and Chien, N. "Similarity of Distorted
    River Models with Movable Beds." Trans. ASCE, Proc.
    Paper No. 2805, Vol 121, 1956.

Henderson, F.M. Open Channel Flow. New York: Macmillan
    Ltd., 1967.

Hydrological Engineering Center. HEC-2 Water Surface
    Profiles Users Manual. Davis, CA.: U.S. Army Corps of
    Engineers, 1976.

Langhaar, H.L. Dimensional Analysis and Theory of Models.
    New York: John Wiley and Sons, Inc., 1951.

MacKay, G.H.
    A Quantitative Study of the Geomorphology of the Wilson
    Creek Watershed, Manitoba. Unpublished M.Sc. thesis,
    University of Manitoba, 1969.

Morris, H.M., and Wiggers, J.M. Applied Hydraulics in
    Engineering, 2nd Edition. New York: The Ronald Press
    Co., 1972.

Olivier, H. "Throughflow and Overflow Rockfill Dams - New
    Design Techniques." ICE Proceedings, Paper No. 7012, Vol
    36, 1967.

Planning Branch. "Committee on Headwater Flood and Erosion Control - Report on Activities in Wilson Creek Watershed April 1, 1976 to March 31, 1977." Winnipeg: Manitoba Department of Mines, Resources and Environmental Management, Water Resources Division, 1977.

-. "Committee on Headwater Flood and Erosion Control - Report on Activities in Wilson Creek Watershed April 1, 1978 to March 31, 1979." Winnipeg: Manitoba Department of Mines, Resources and Environmental Management, Water Resources Division, 1979.

Raudrivi, A. Loose Boundary Hydraulics. Oxford: Pergamon Press, Ltd., 1976.

Richardson, E.V., Simons, D.B., Karaki, S., Mahmood, K., and Stevens, M.A. Highways in the River Environment Hydraulic and Environmental Design Considerations. Fort Collins, CO.: U.S. Department of Transportation, Federal Highway Administration, 1975.

Sharp, J.J. Hydraulic Modelling. London: Butterworth & Co., Ltd., 1981.

Smith, C.D. Hydraulic Structures. Saskatoon: University of Saskatchewan Press, 1978.

Stephenson, David. Rockfill in Hydraulic Engineering. New York: Elsevier Scientific Publishing Co., 1979.

Strilaeff, P.W. The Riding Mountain - Westlake Record Storm and Flood of September 1975. Water Survey of Canada, Atmospheric Environment Service and Manitoba Department of Mines, Resources and Environmental Management, 1976.

Yalin, M.S. Theory of Hydraulic Models. London: The MacMillan Press Ltd., 1971.

Yalin, M.S. Mechanics of Sediment Transport. Oxford: Pergamon Press, Ltd., 1977.

Appendix A

FIGURES

DAUPHIN LAKE

DAUPHIN

TURTLE
RIVER

RIDING MOUNTAIN
NATIONAL PARK

WILSON CREEK
EXPERIMENTAL
WATERSHED

NEEPAWA

BRANDON

0   10   20   km

SCALE
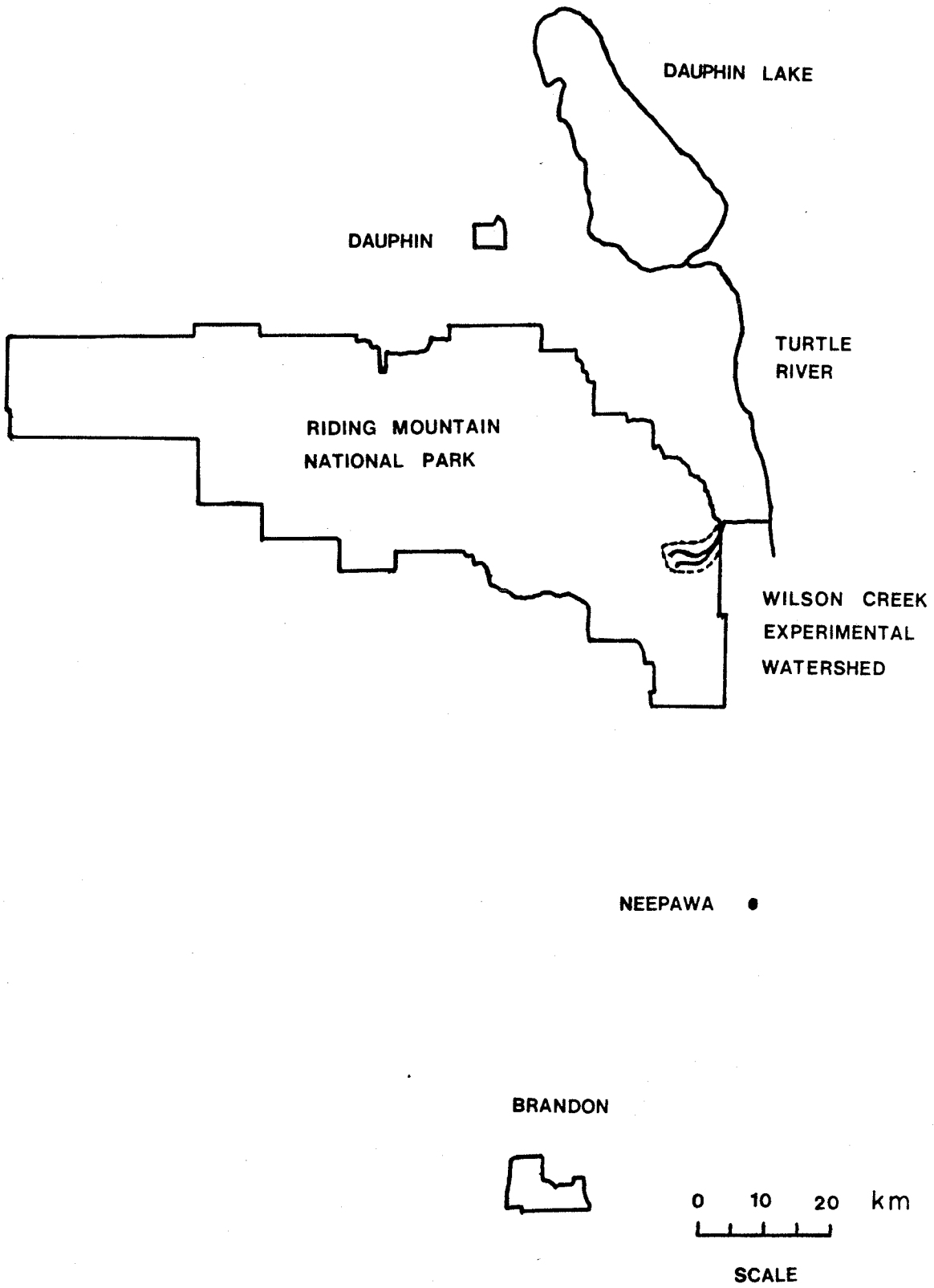
Figure 1.1   General Layout Plan – Manitoba Escarpment Region
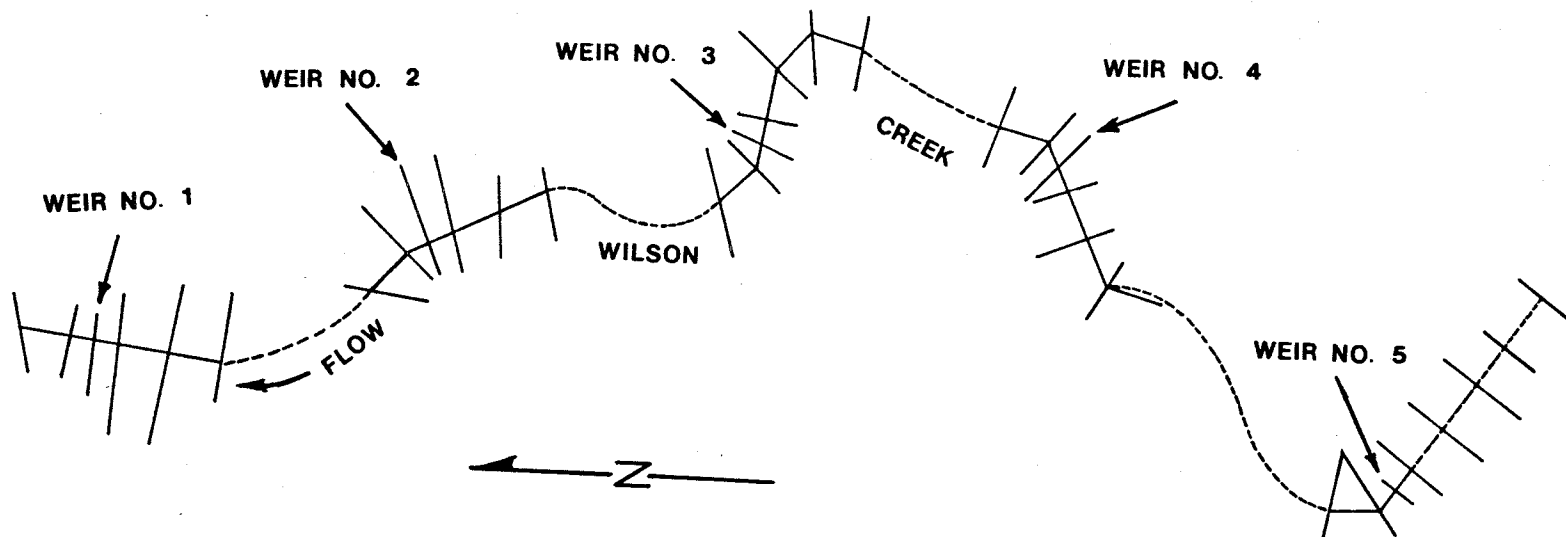
Figure 1.2   General Layout of Prototype Structures

WEIR NO. 1

EXISTING PRAIRIE

WEIR NO. 2

WEIR NO. 3

S = 0.0095

WEIR NO. 4

WEIR NO. 5

ELEVATION m

345

340

335

330

325

1600   1400   1200   1000   800   600   400   200

STATION   m
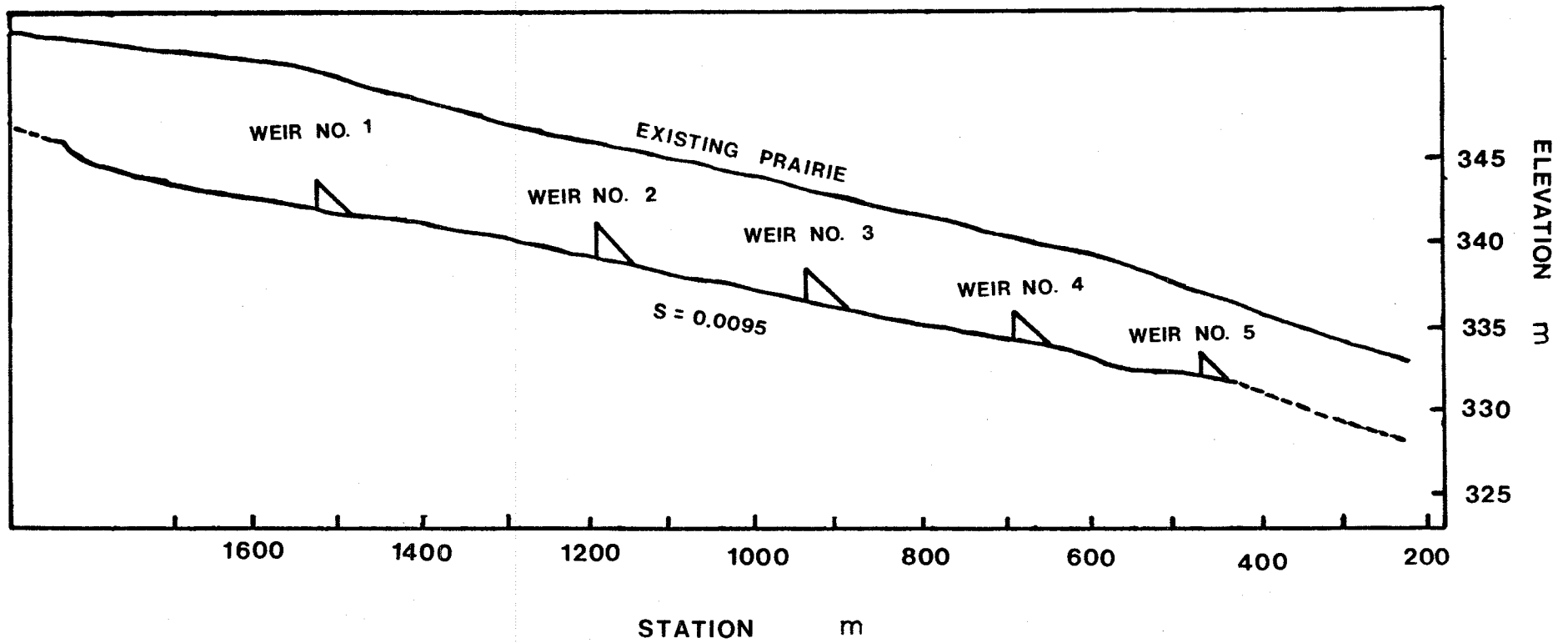
Figure 1.3   Profile of Prototype Bed

82
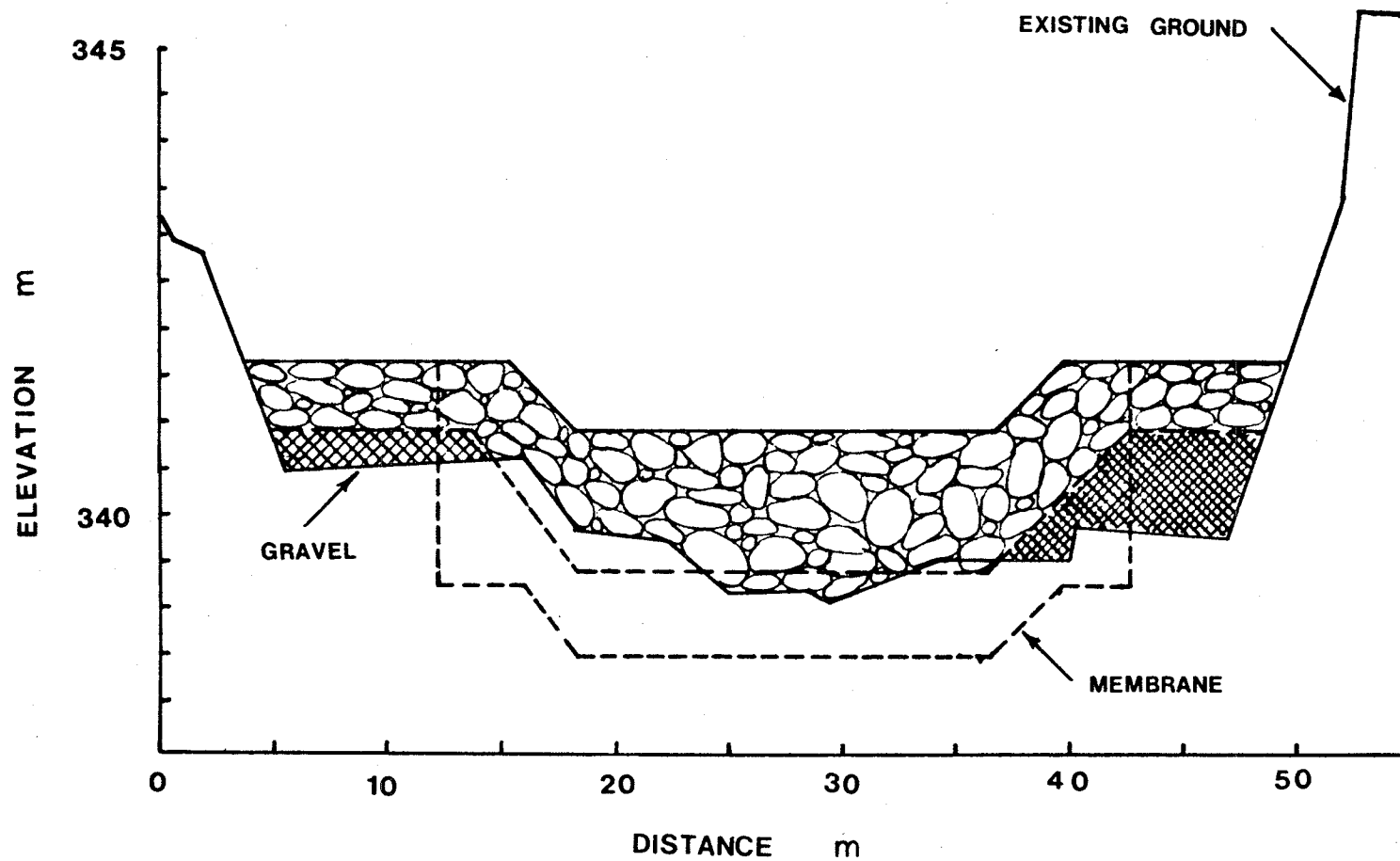
Figure 1.4   Prototype Crest Cross Section
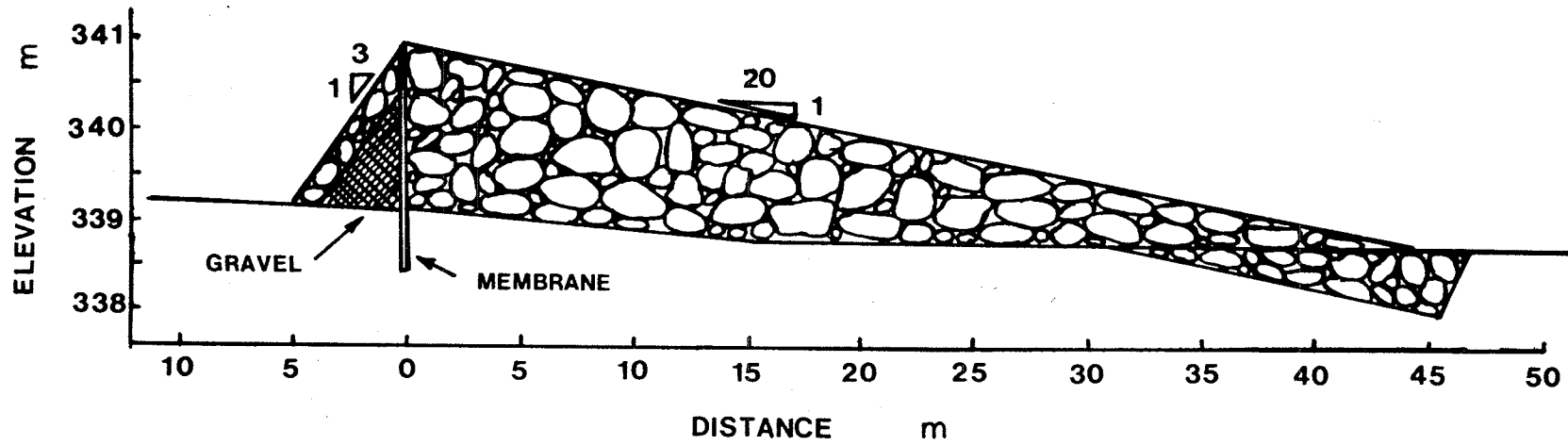
Figure 1.5   Prototype Weir Profile
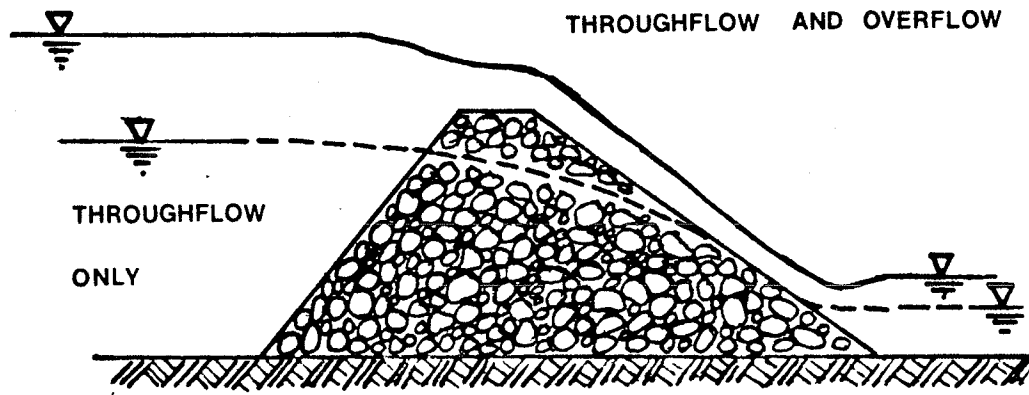
Figure 2.1 Throughflow and Overflow in Rockfill Weirs
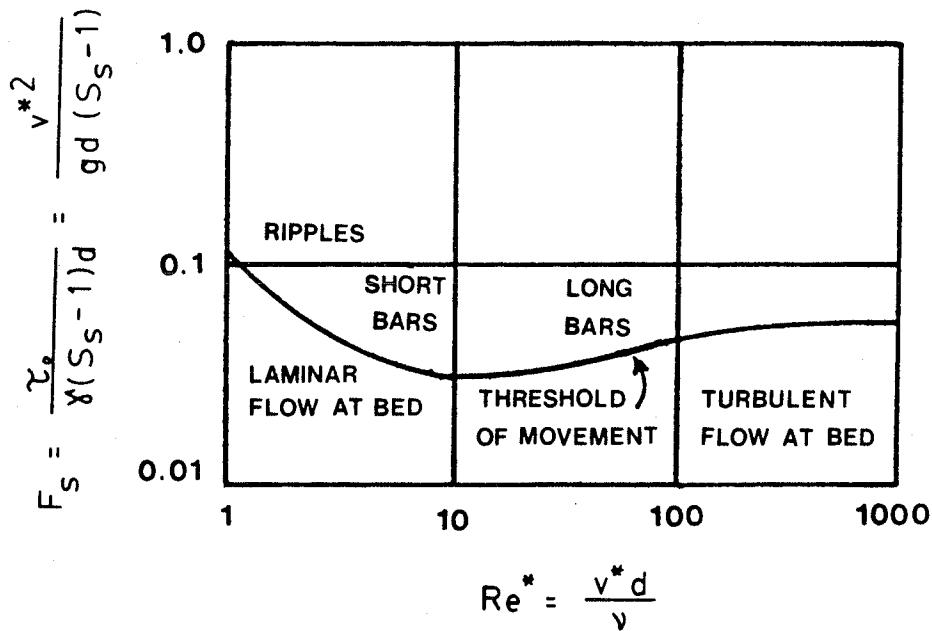
Figure 2.2 Shields Entrainment Function
(after Henderson)
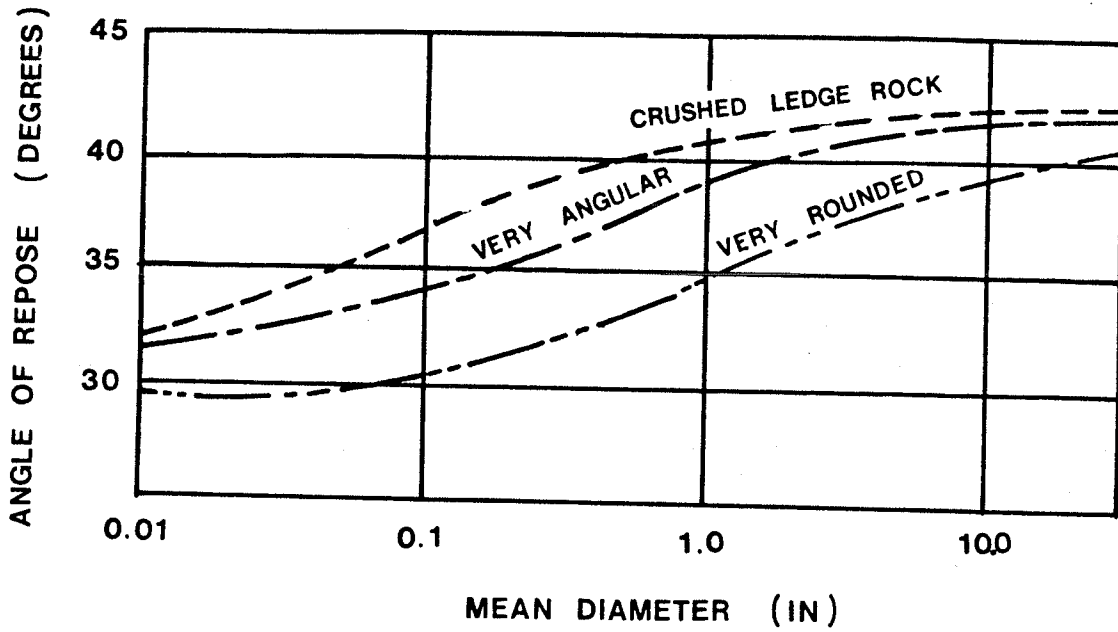
Figure 2.3   Angle of Repose for Dumped Riprap
(after Richardson et al)
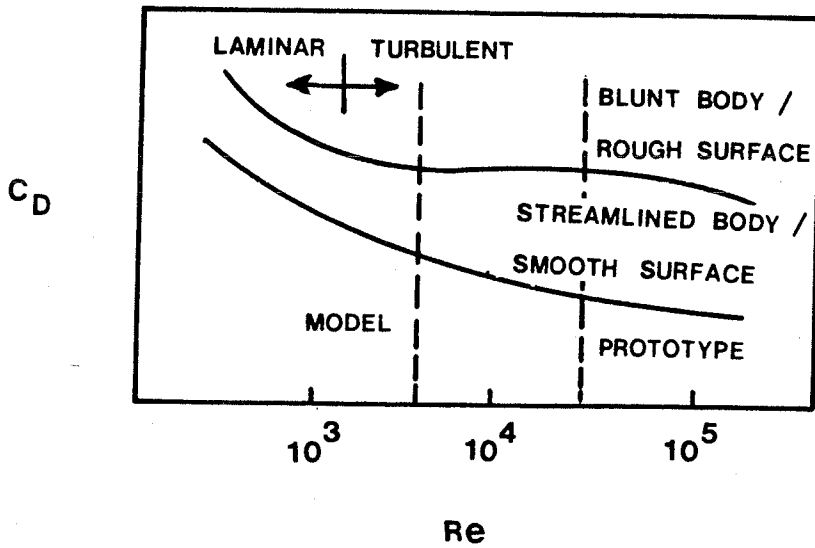
Figure 3.1   Effect of Reynolds Number on Drag Coefficient
(after Henderson)
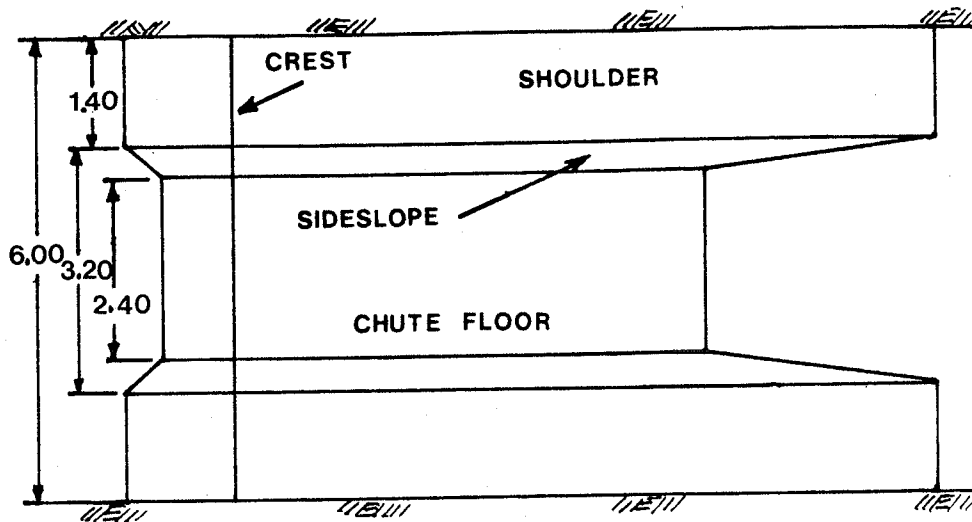
(a) PLAN

all dimensions in m
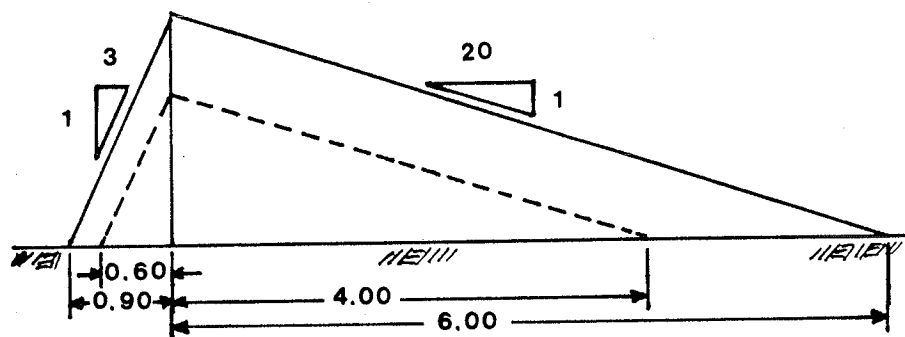
(b) PROFILE

Figure 4.1 Simplified Weir Geometry - Model

all dimensions in m
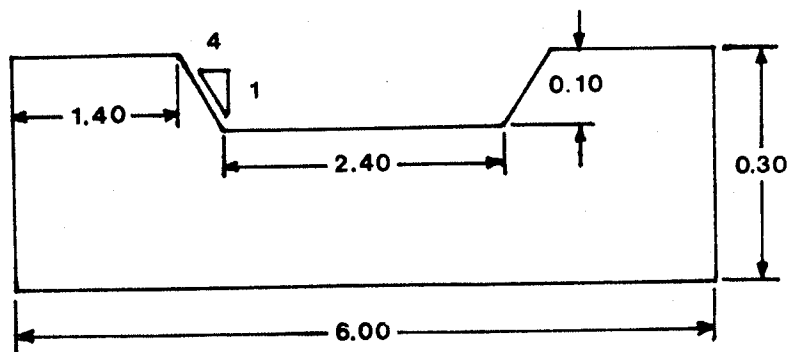
Figure 4.2 Cross Section Through Model Crest
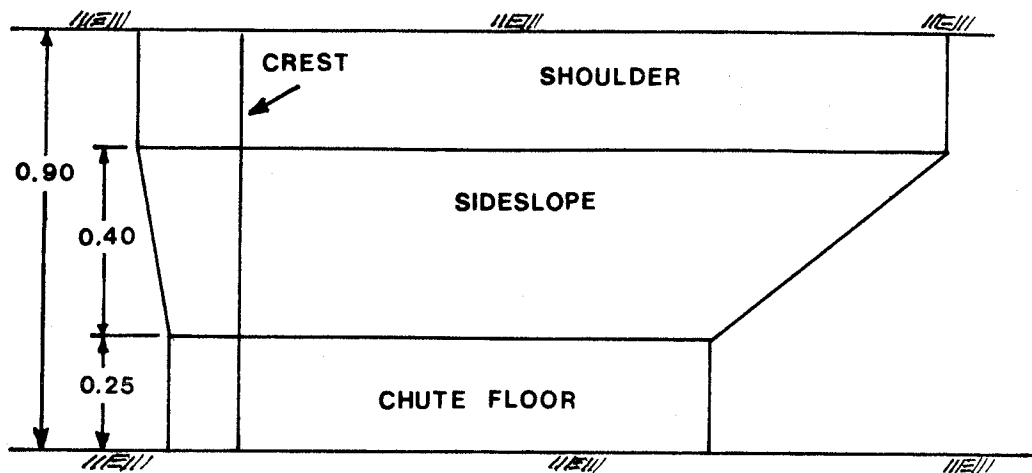
(a) PLAN
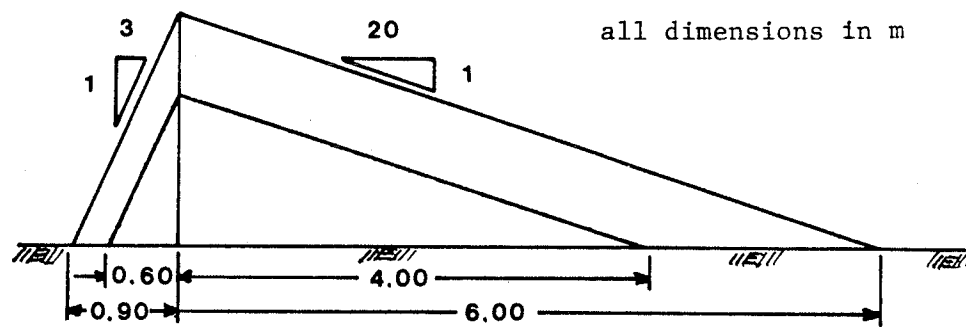
(b) PROFILE
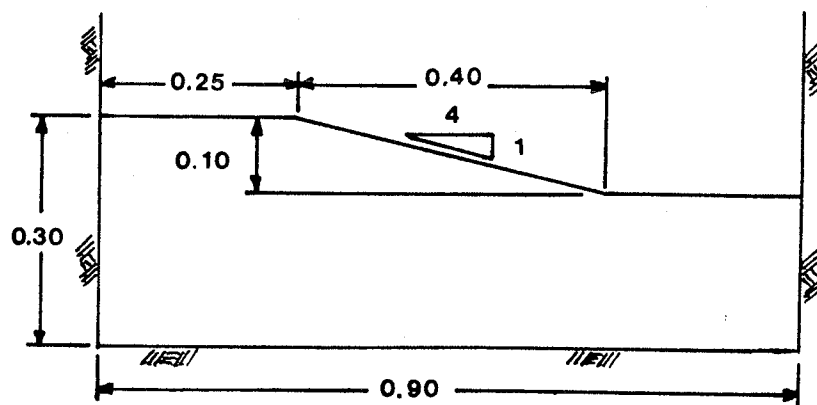
all dimensions in m

(c) CROSS SECTION THROUGH CREST

Figure 4.3   Geometry of Three Dimensional Model
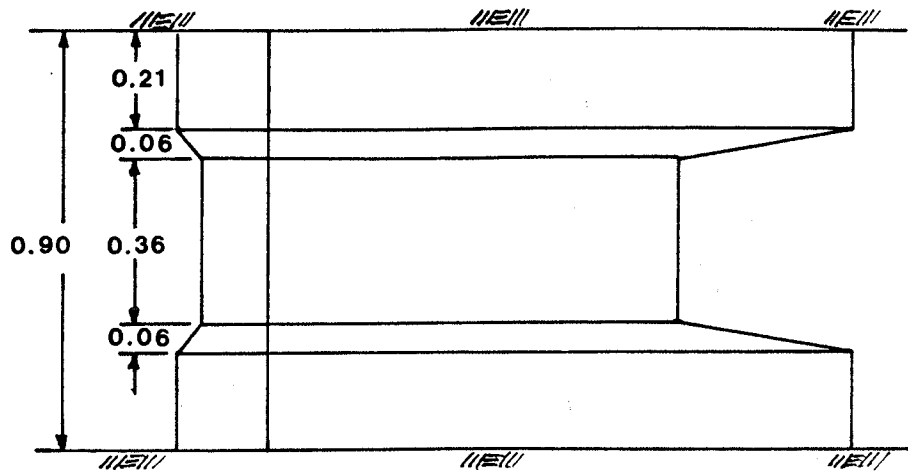
(a) PLAN

all dimensions in m
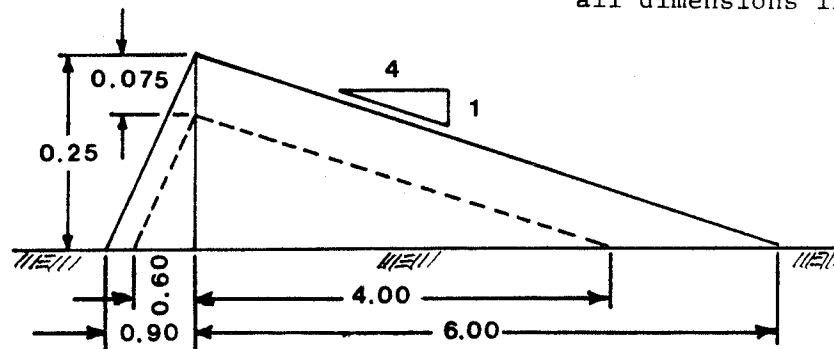
(b) PROFILE

Figure 4.4   Distorted Model Geometry
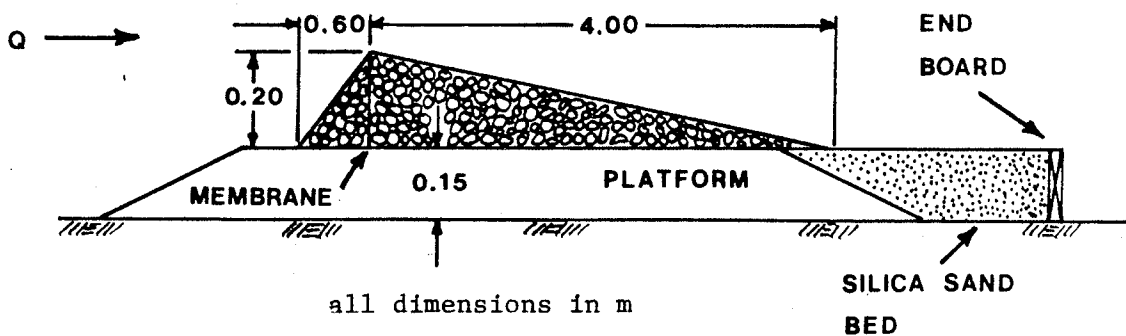
all dimensions in m

Figure 4.5   Profile Through Center Line of Two Dimensional Model
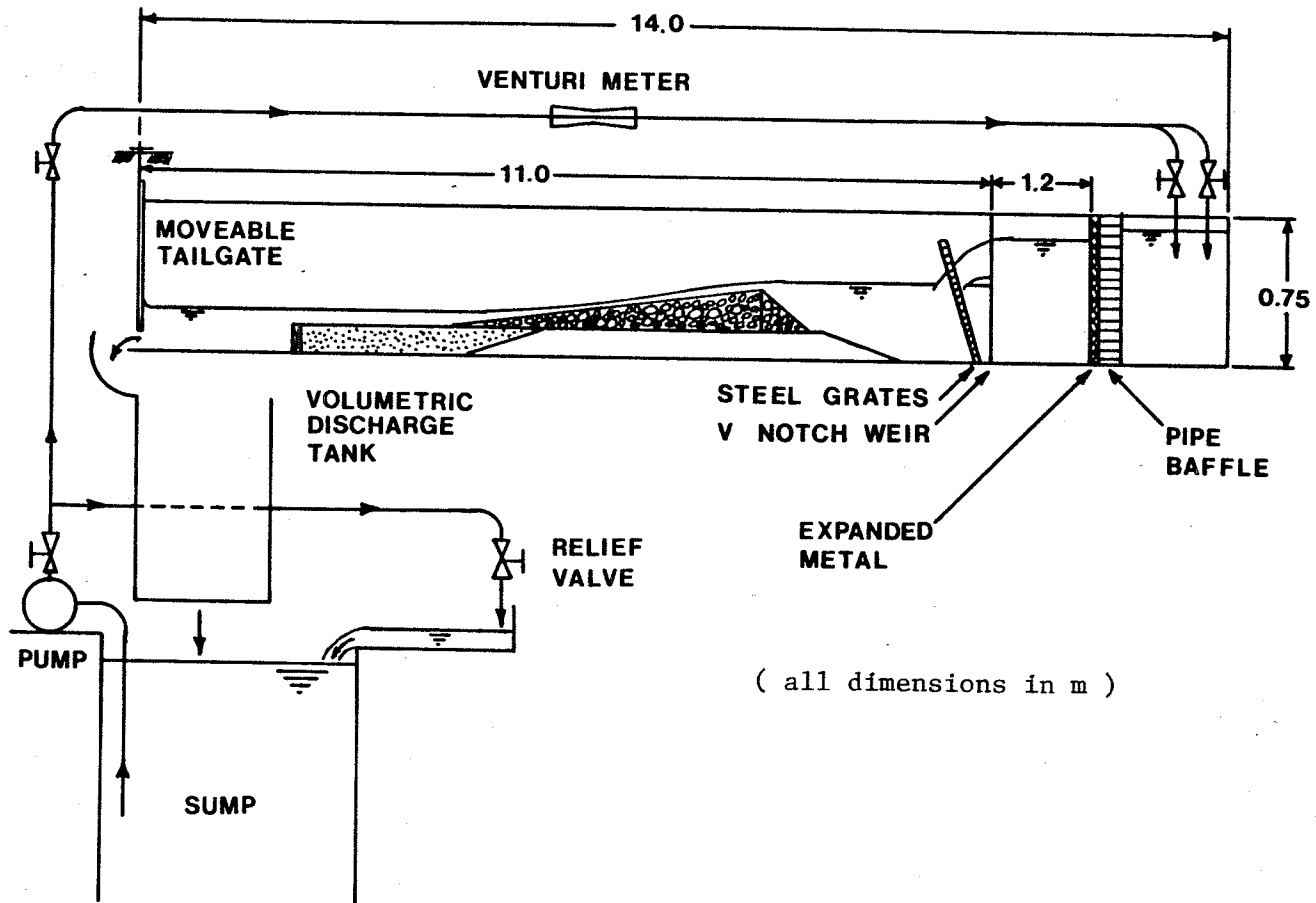
(all dimensions in m)

Figure 4.6   Laboratory Facilities

$q \ m^2/s \times 10^{-3}$

HEAD ON CREST cm

2

1

$Q_2 \ m^3/s \times 10^{-3}$

1.20   0.40   1.40

11 cm   10 cm

0.25

① ② ③

0.90
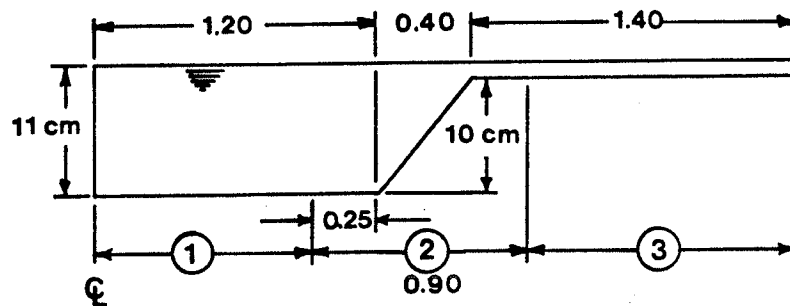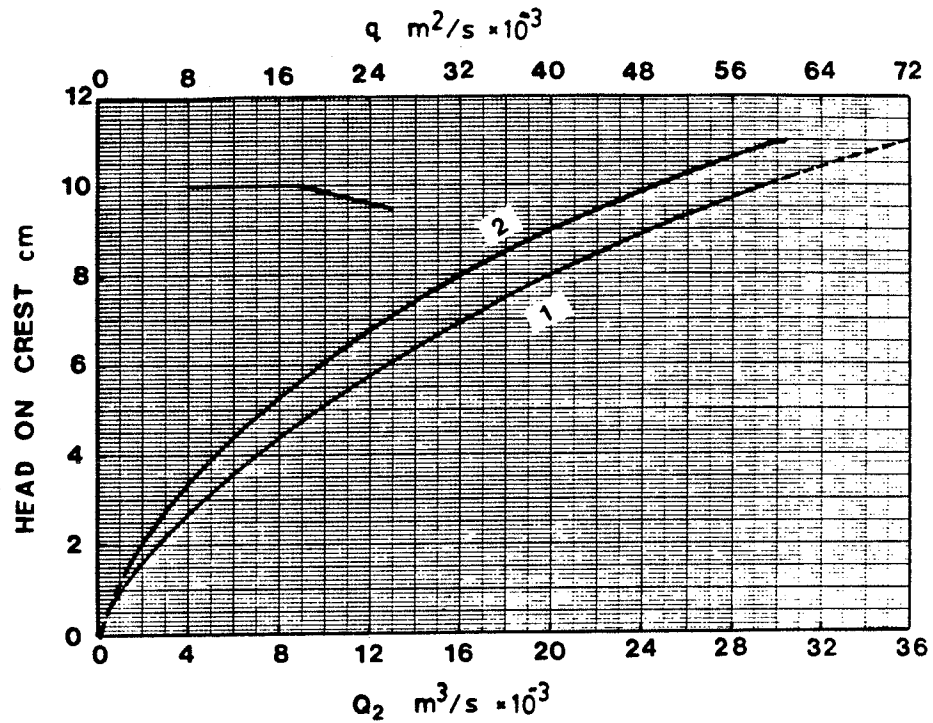
(all dimensions in m unless noted)

Q_2 sideslope model (area 2) discharge @ h=11 cm .... <u>30.5 1/s</u>

remaining crest length (length 1) in chute ...... 0.95 m

unit discharge in sectional model (curve 1)
@ h=11 cm ..... 72 $m^2/s \ x10^{-3}$

Q_1 discharge over length 1   0.95 x 72 = <u>68.4 1/s</u>

remaining crest length over shoulder (length 3)   1.15 m

unit discharge in sectional model (curve 1)
@ h=1 cm ...... 1 $m^2/s \ x10^{-3}$

Q_3 discharge over length 3   1.15 x 1 = <u>1.2 1/s</u>

Total discharge $Q_1 + Q_2 + Q_3$ = 68.4 + 30.5 + 1.2 = 100.1 1/s
(one side)

Total discharge (both sides)   = 100.1 x 2 = <u>200.2 1/s</u>

Figure 4.7   Rating Curve Development
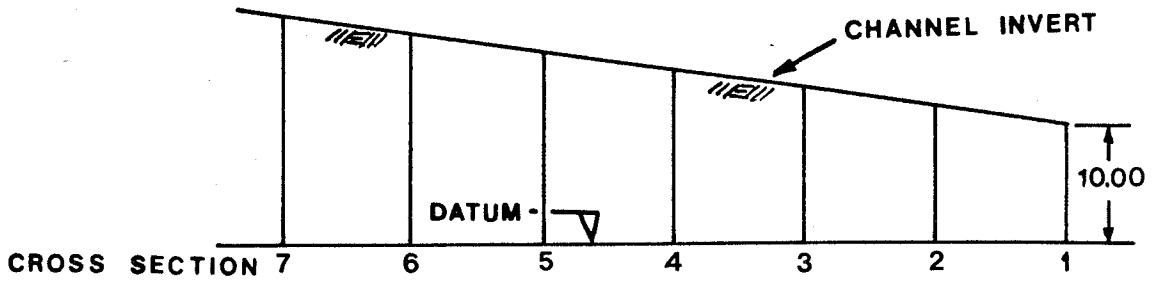
(a) PROFILE

(all dimensions in m)
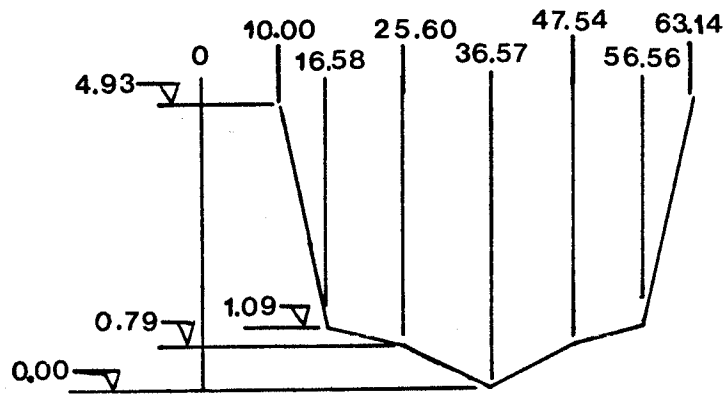
(b) CROSS SECTION

CROSS SECTION	STATION (m)	ELEVATION OF INVERT (m)
1	0.00	10.00
2	166.67	11.58
3	333.32	13.17
4	500.00	14.75
5	667.67	16.34
6	834.34	17.93
7	1000.00	19.50

Figure 4.8   Simplified Channel Geometry - HEC 2 Series A

(a) PROFILE
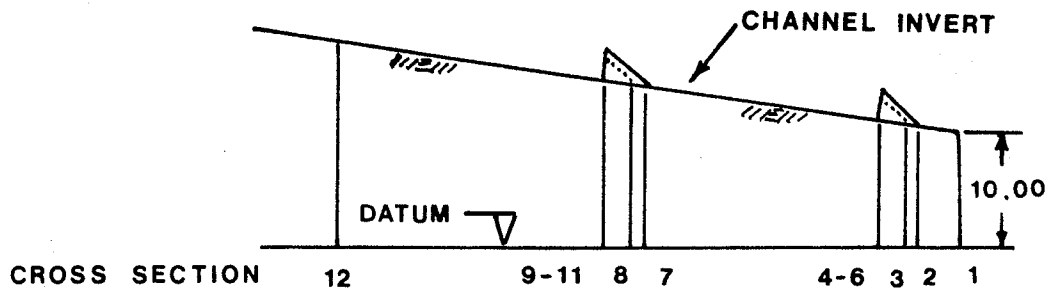
(all dimensions in m)
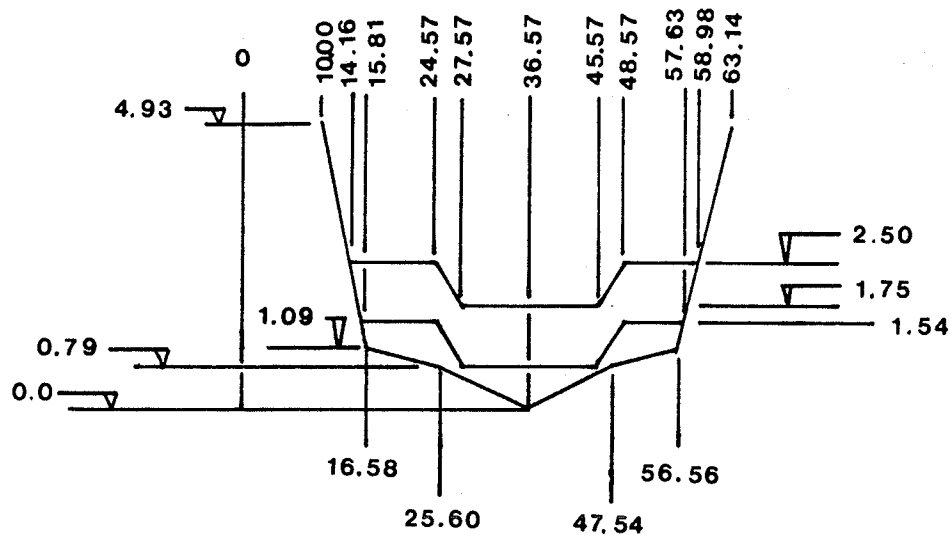
(b) CROSS SECTION

CROSS SECTION	STATION (m)	ELEVATION OF INVERT (m)
1	0.00	10.00
2	58.52	10.56
3	76.30	10.72
4	100.00	10.95
5	102.80	10.98
6	104.90	11.00
7	408.52	13.88
8	426.30	14.05
9	450.00	14.28
10	452.80	14.30
11	454.90	14.32
12	800.00	17.60

Figure 4.9   Simplified Channel and Weir Geometry – HEC 2 Series B
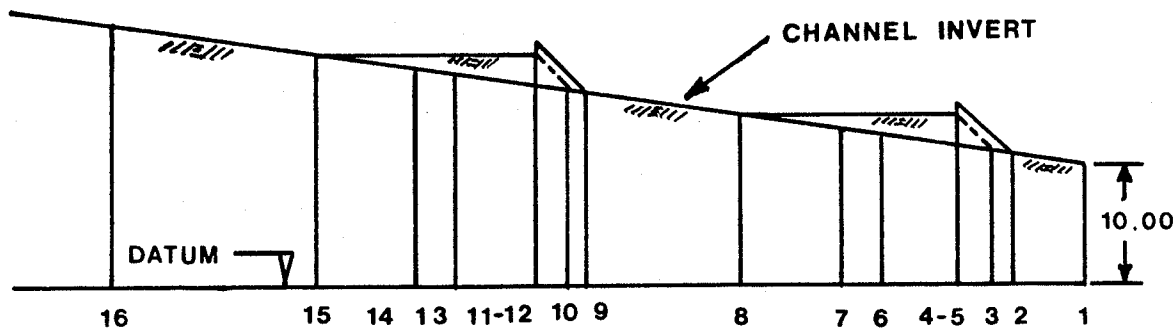
(a) PROFILE

(all dimensions in m)
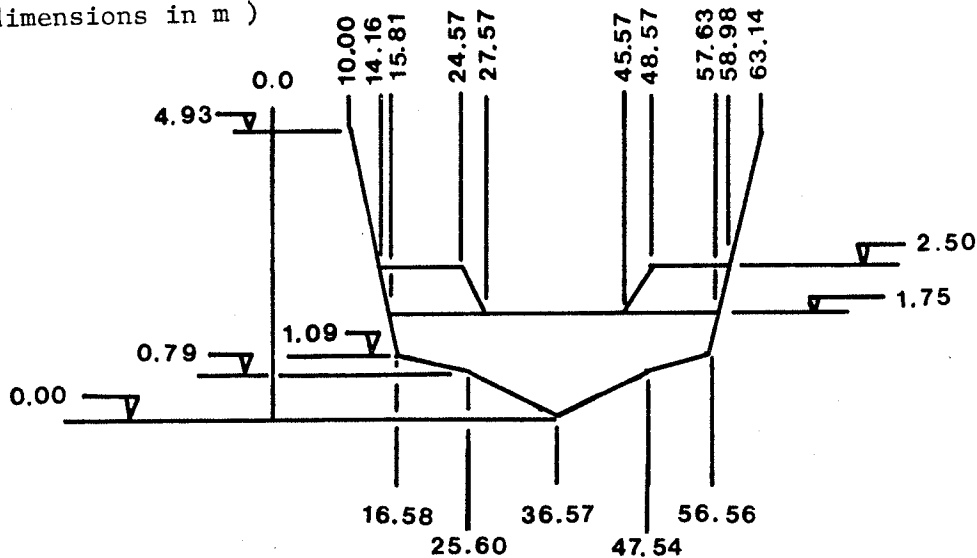
(b) CROSS SECTION

CROSS SECTION	STATION (m)	ELEVATION OF INVERT (m)
1	0.00	10.00
2	58.52	10.56
3	76.83	10.73
4	100.00	10.95
5	102.25	10.97
6	169.47	11.61
7	201.05	11.91
8	284.21	12.70
9	408.52	13.88
10	426.30	14.05
11	450.00	14.28
12	452.25	14.30
13	519.47	14.93
14	551.05	15.23
15	634.21	16.02
16	800.00	17.60

Figure 4.10   Simplified Channel and Weir Geometry - HEC 2 Series C
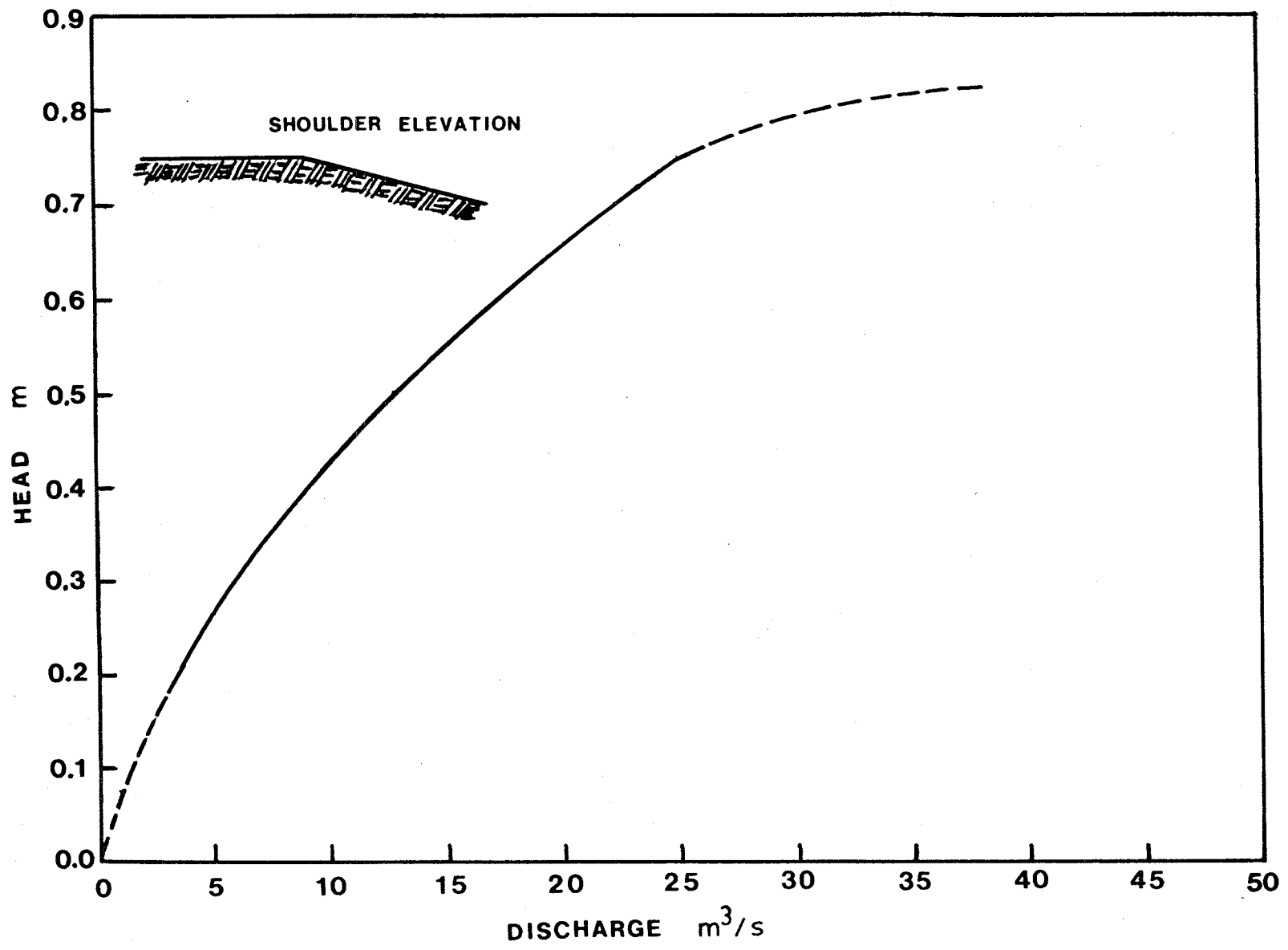
Figure 5.1   Prototype Rating Curve
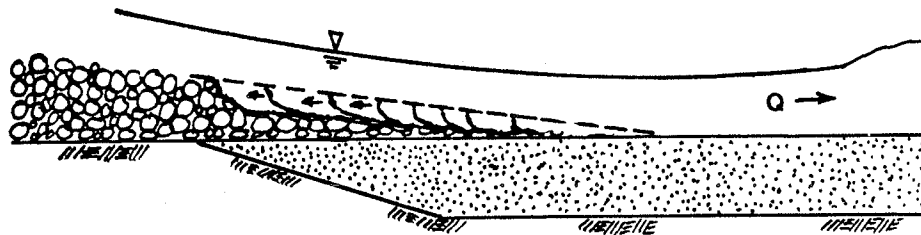
(a) PROFILE

all dimensions in m
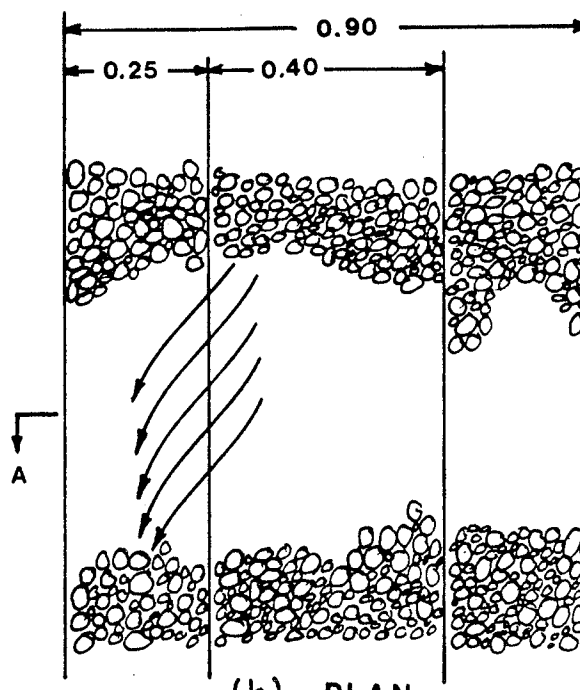
(b) PLAN
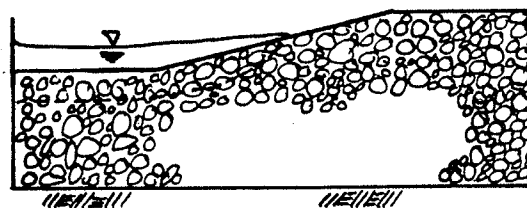
(c) CROSS SECTION A-A

Figure 5.2 Failure Mode
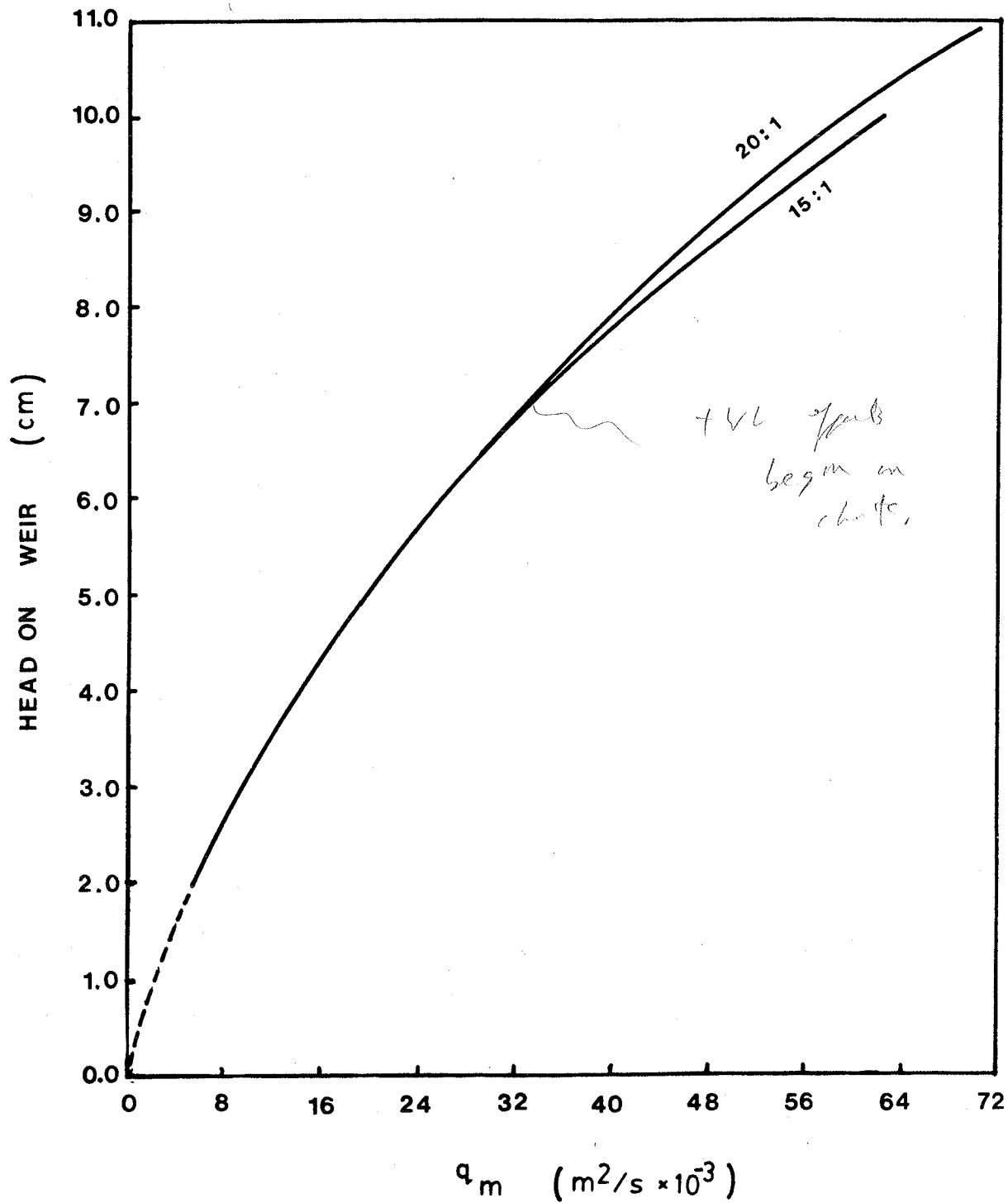
Figure 5.3   Effect of Downstream Slope on Model Rating Curve
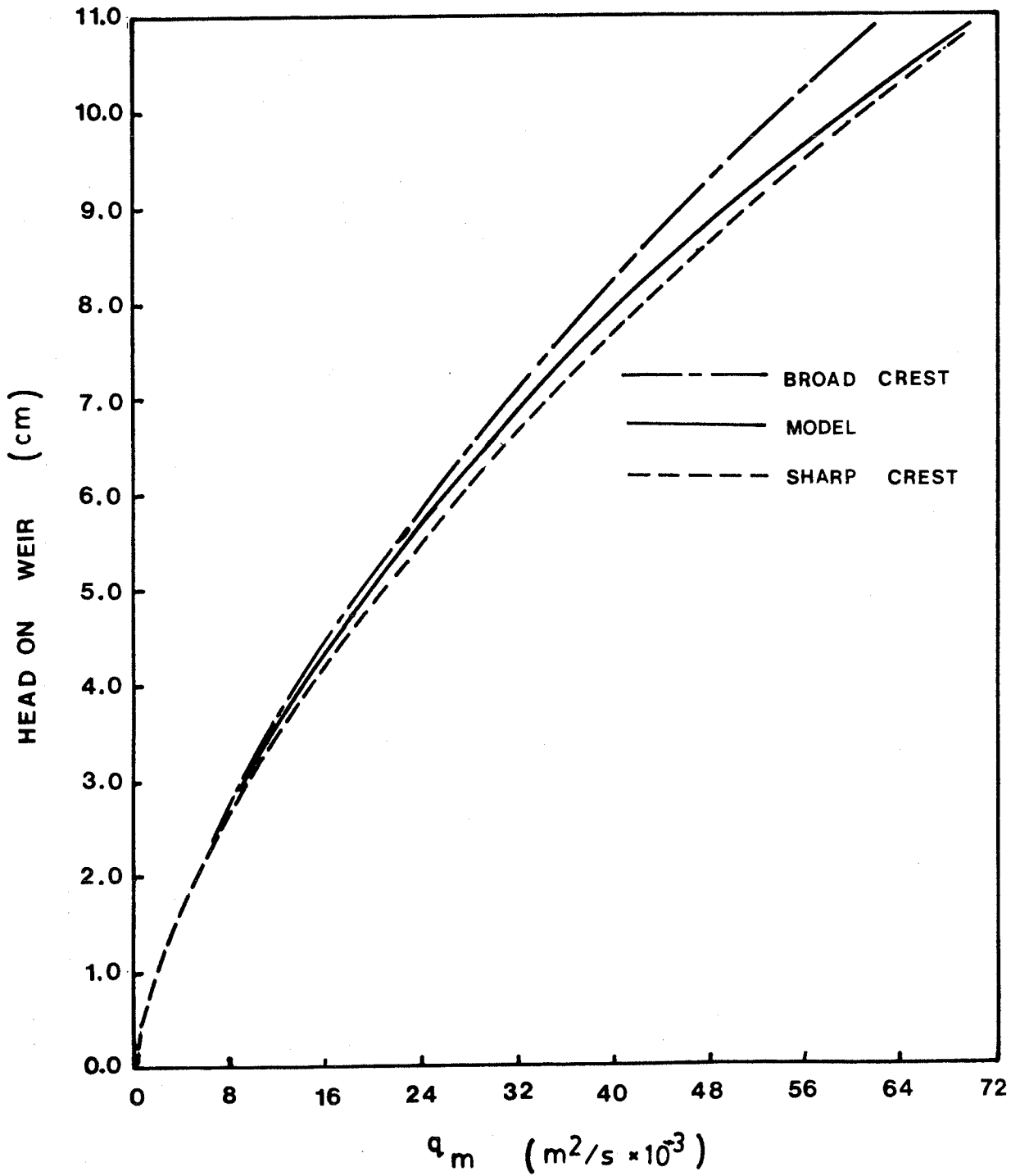
Figure 5.4 Comparison of Model Rating Curve with Broad Crested and Sharp Crested Weirs
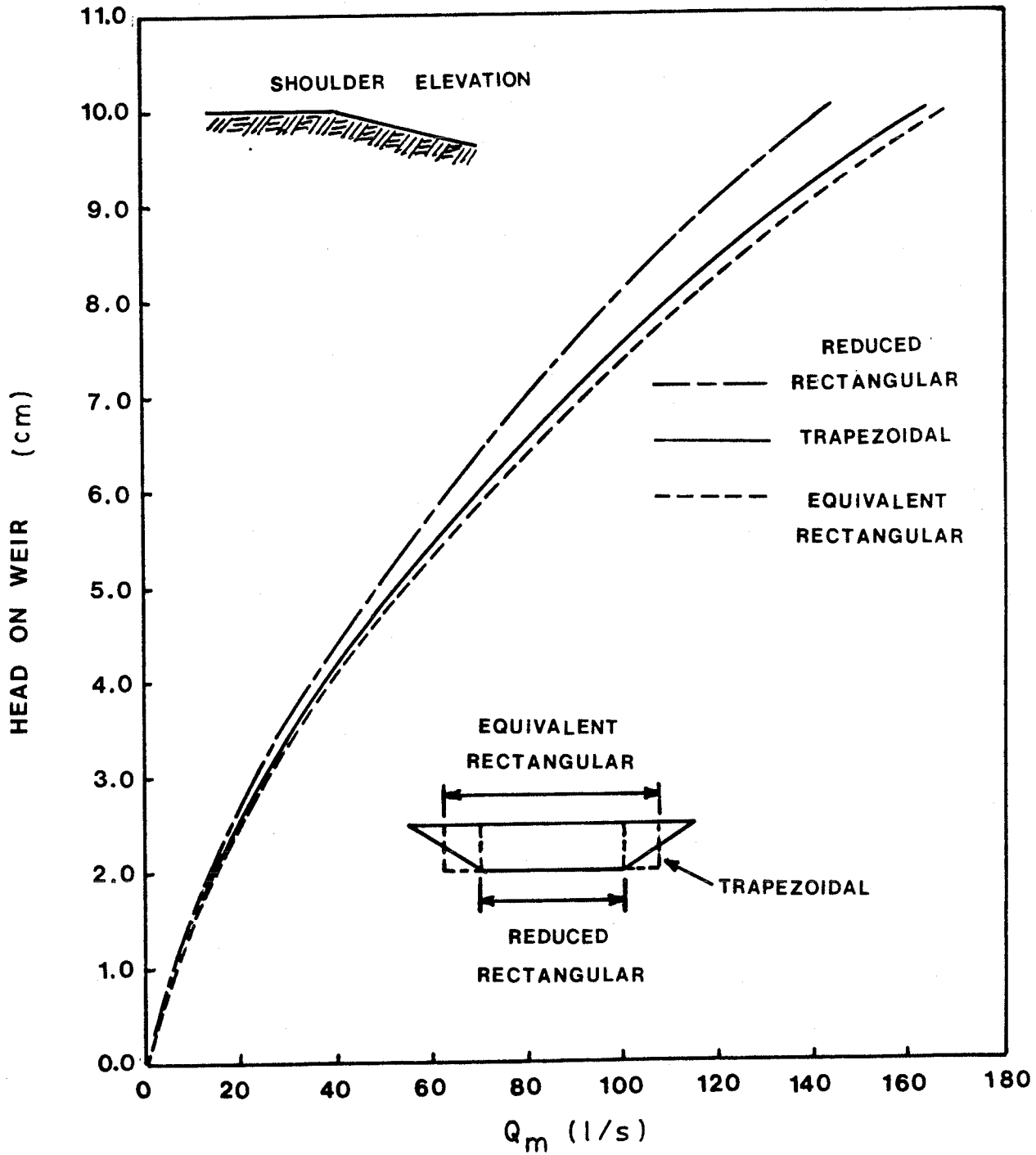
Figure 5.5   Effect of Chute Cross Section on Model Rating Curve
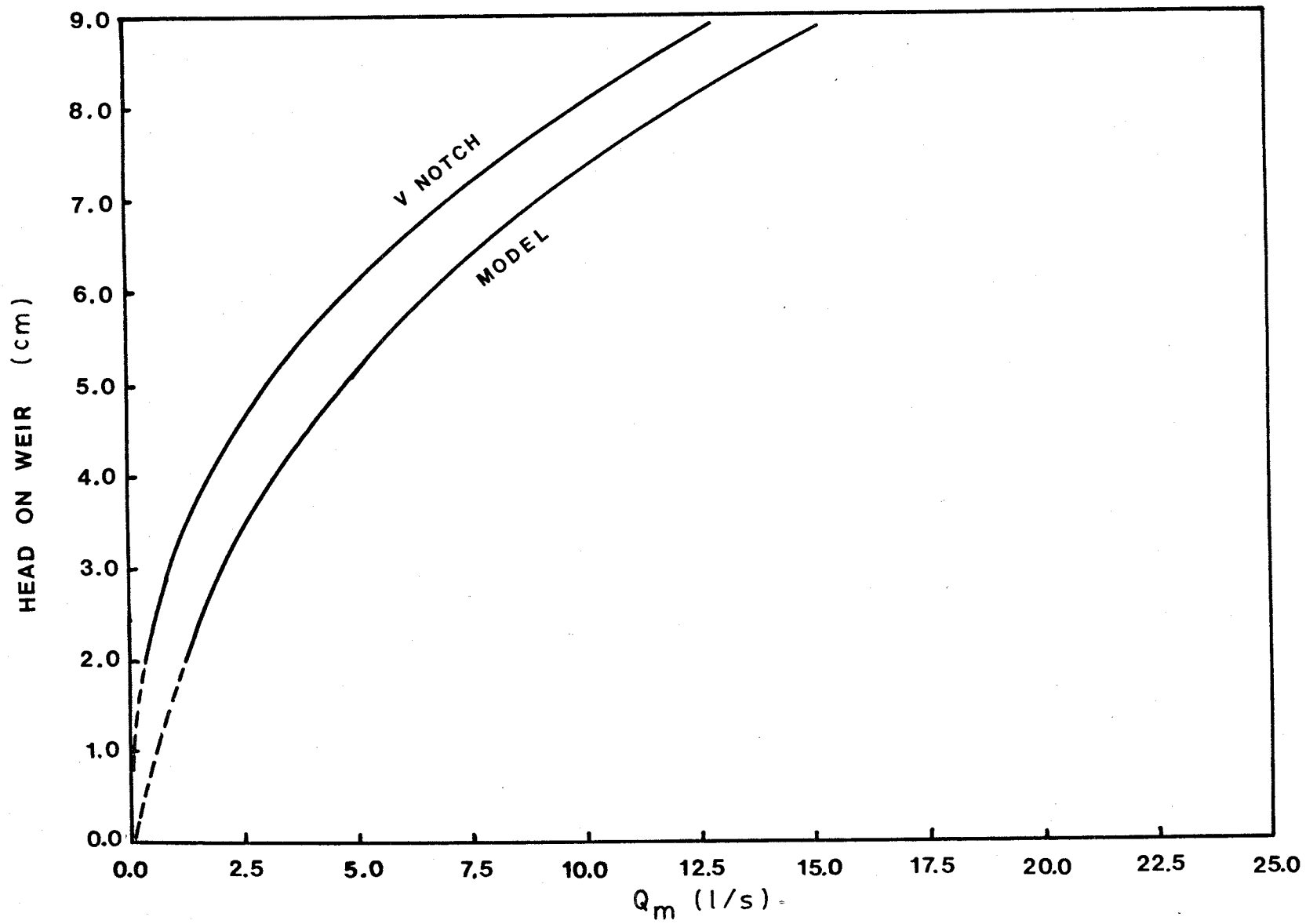
Figure 5.6   Comparison of Shoulder Flow with V Notch Weir Flow
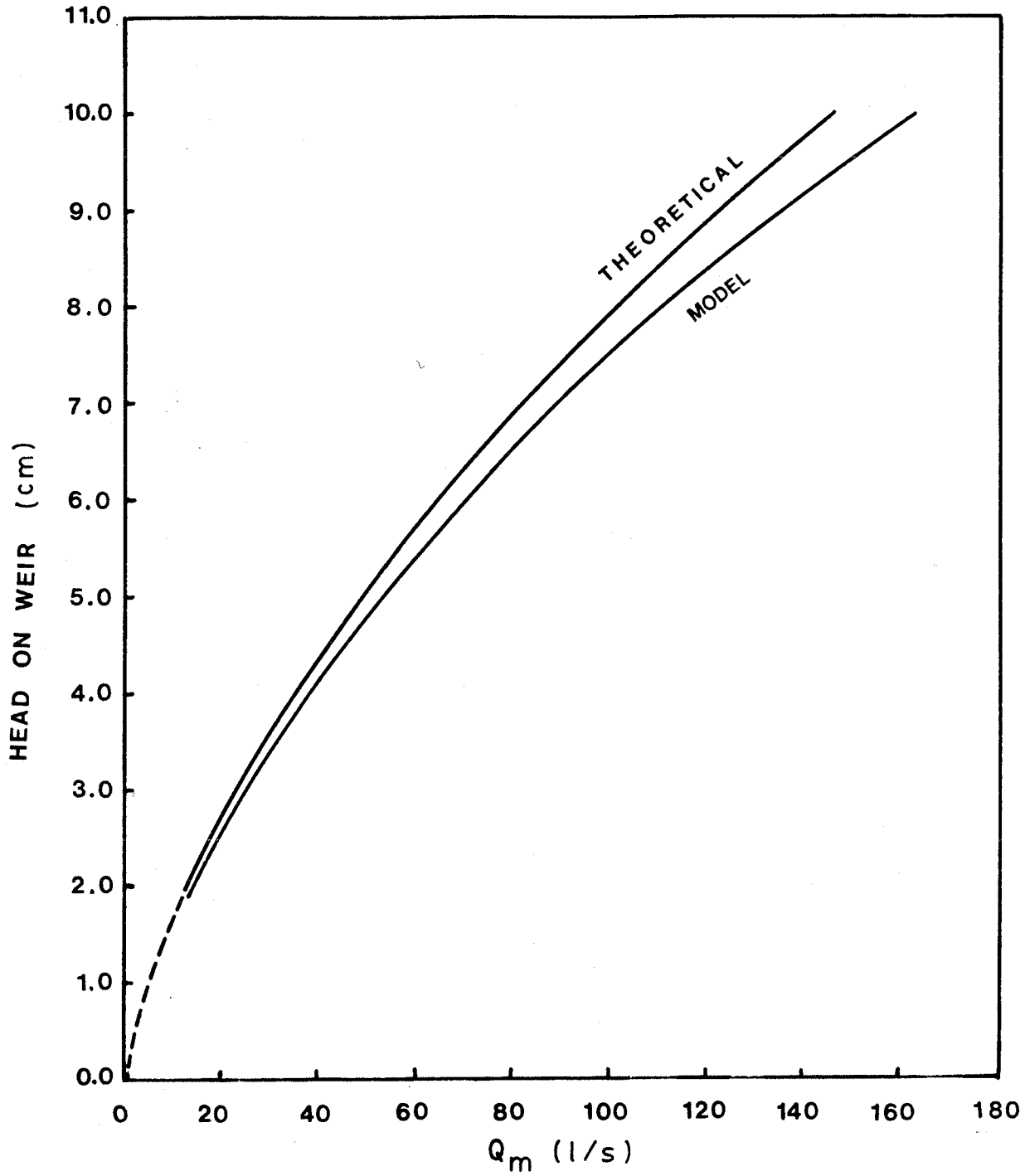
Figure 5.7   Comparison of Model Rating Curve with Theoretical
Trapezoidal Rating Curve
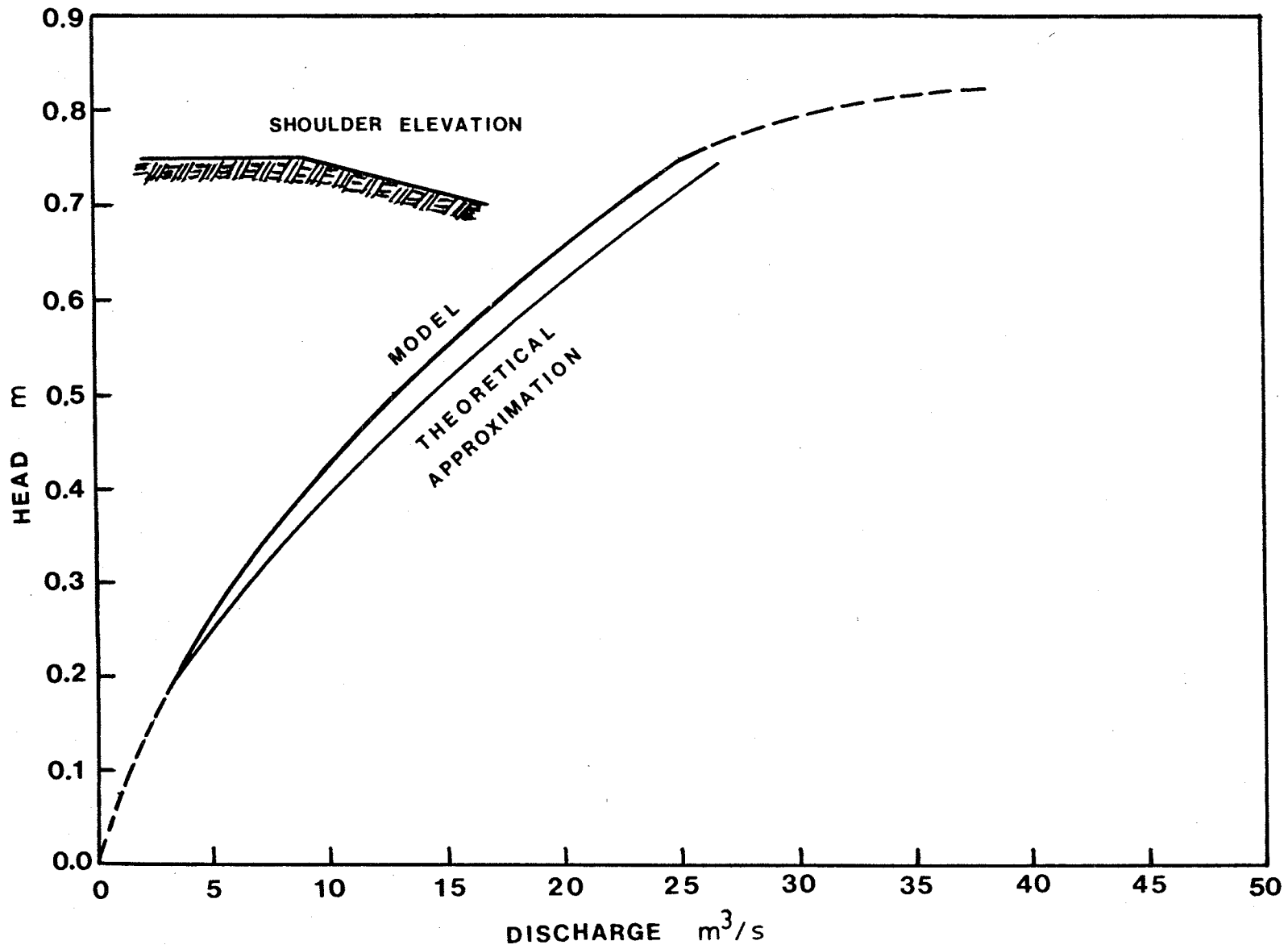
Figure 5.8   Comparison of Prototype Rating Curves from Model and Recommended
Theoretical Approximation
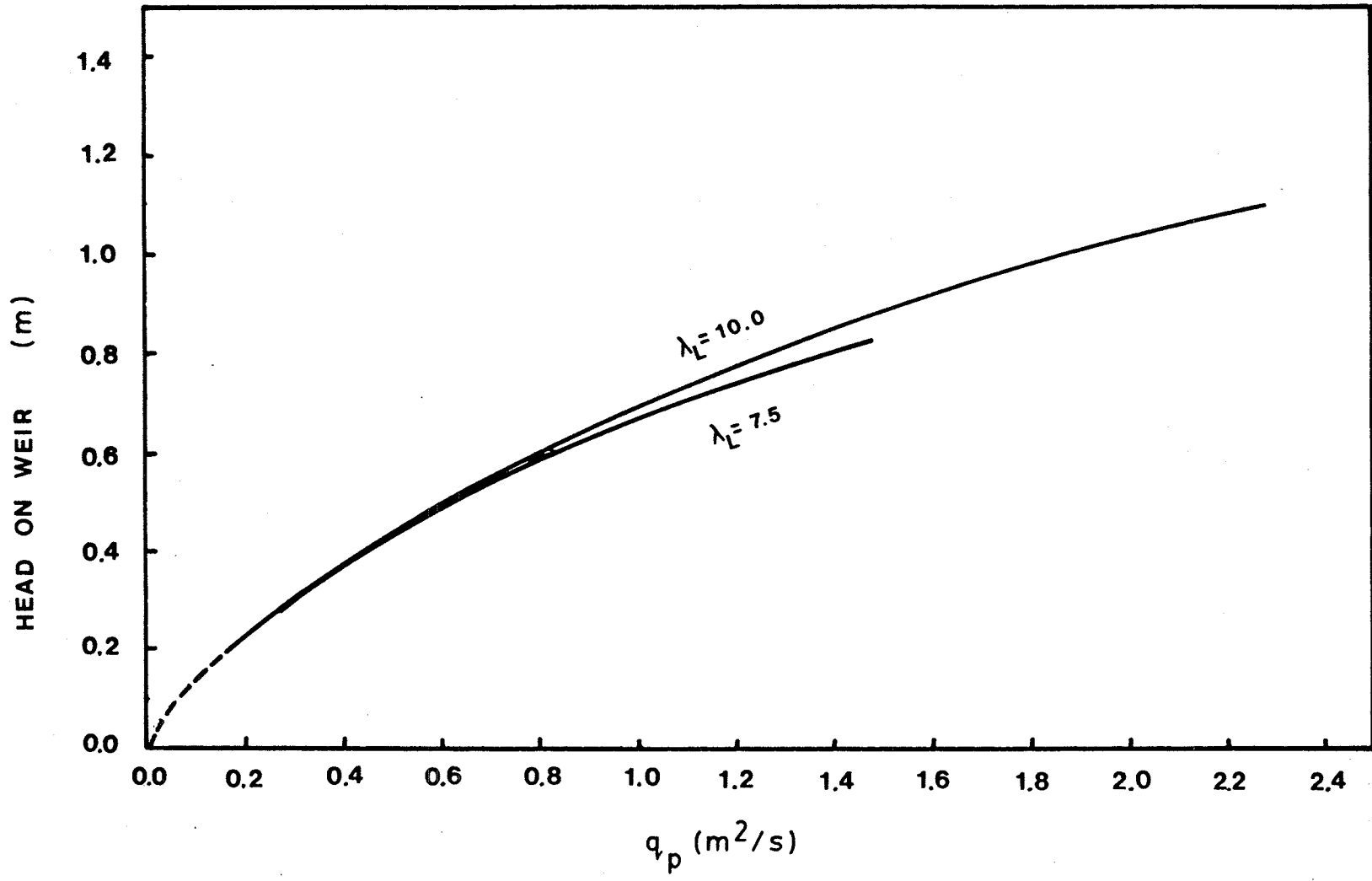
Figure 5.9 Effect of Length Scale on Prototype Rating Curve
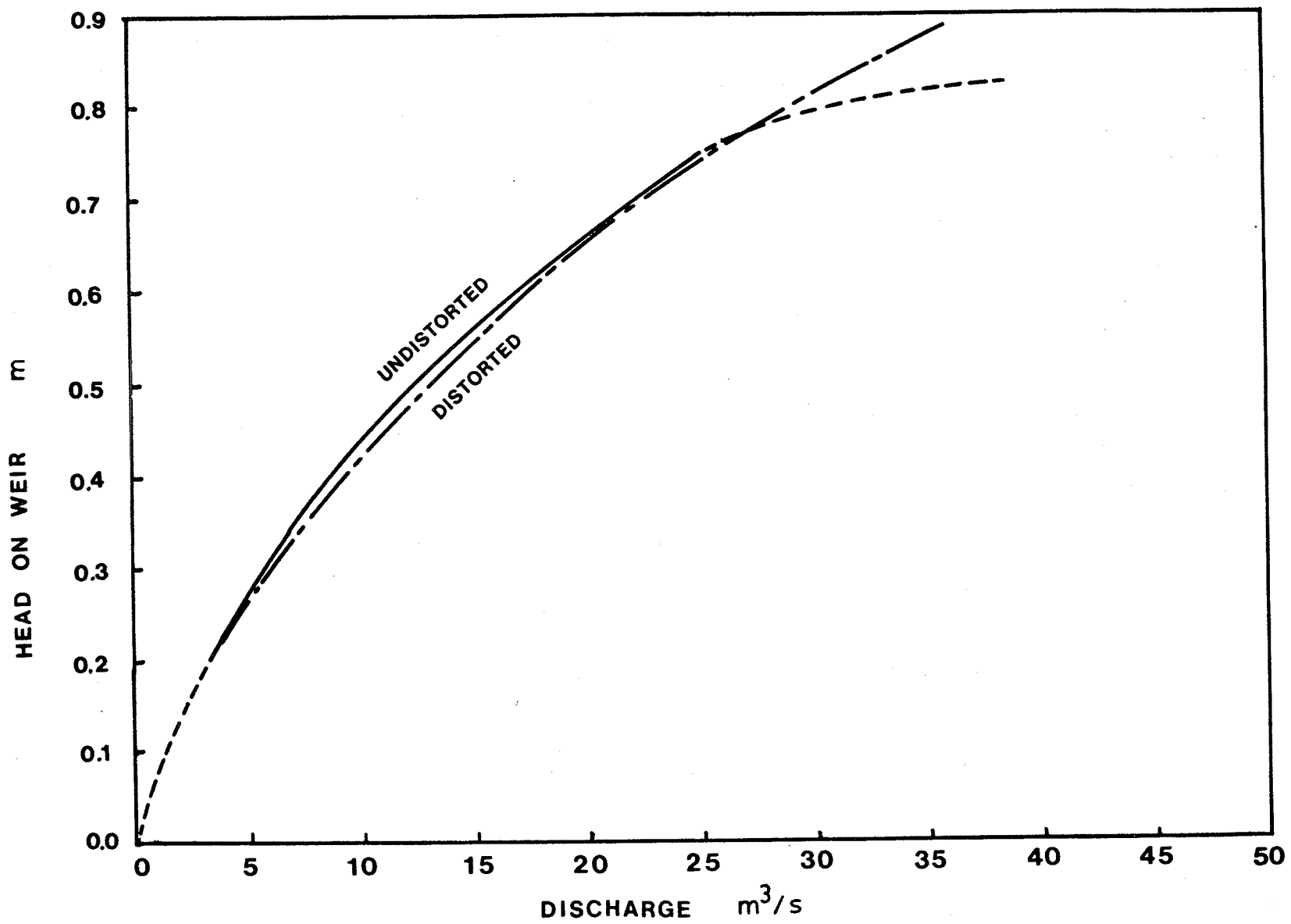
Figure 5.10   Effect of Scale Distortion on Prototype Rating Curve
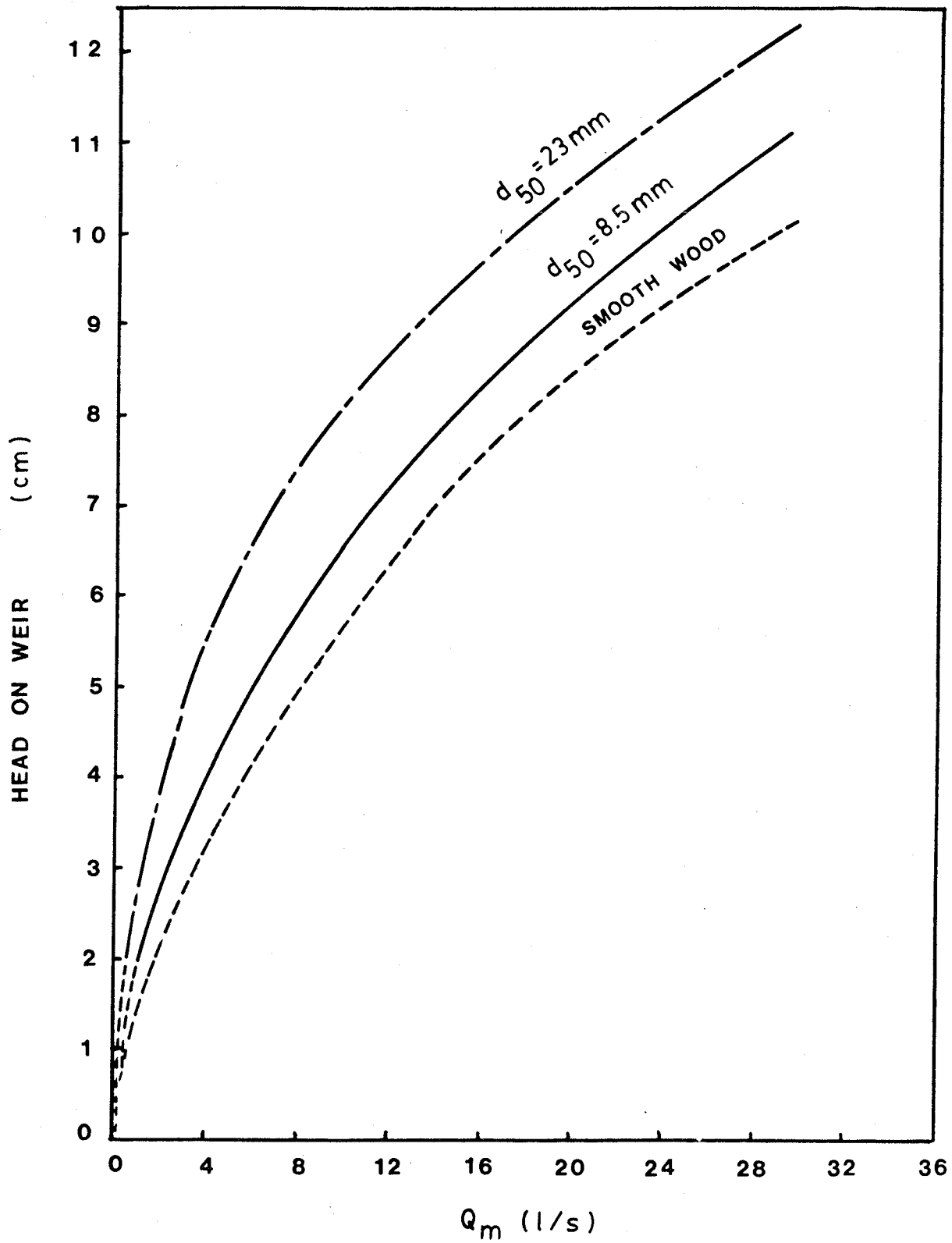
Figure 5.11   Effect of Roughness on Model Rating Curve
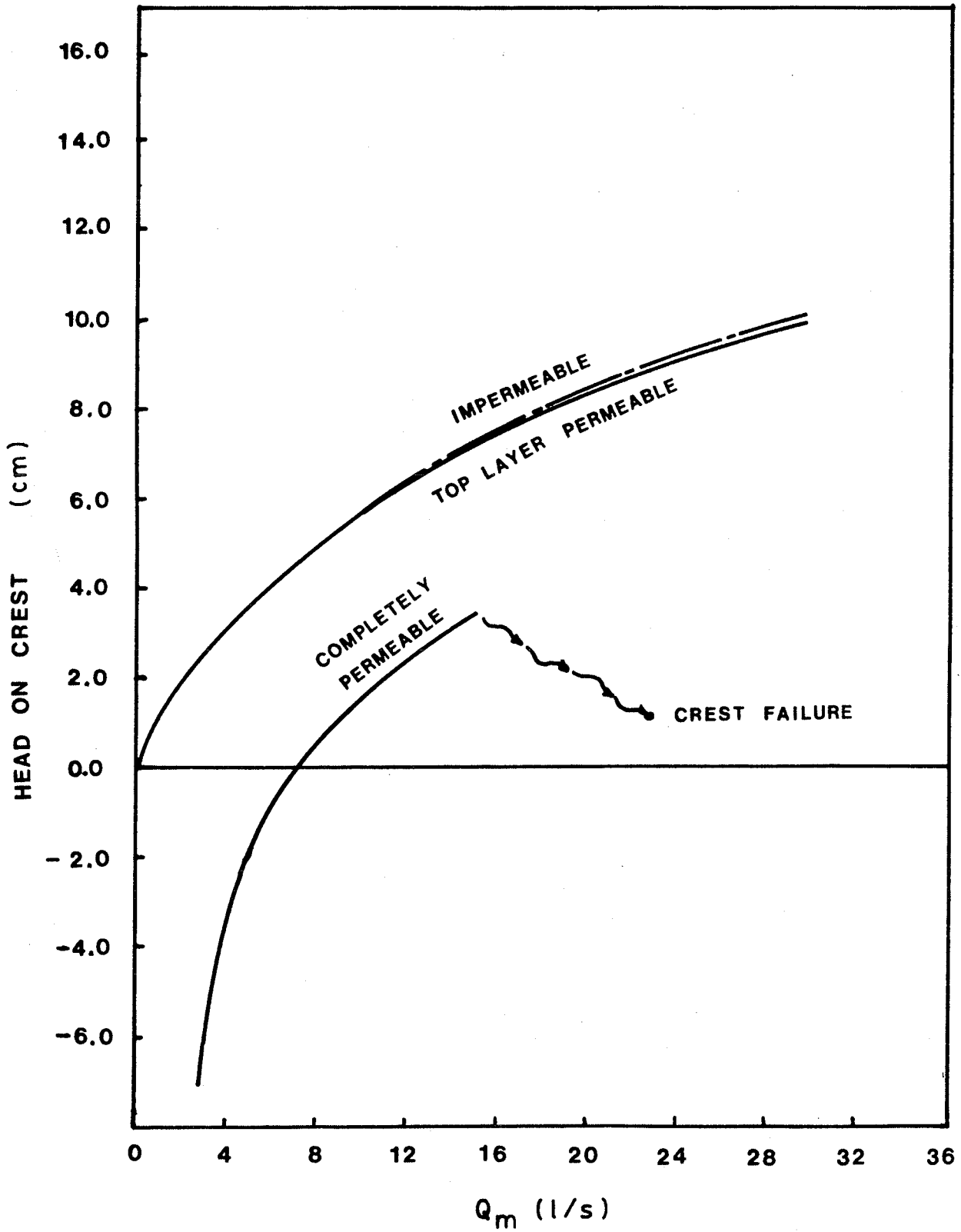
Figure 5.12   Effect of Permeability on Model Rating Curve
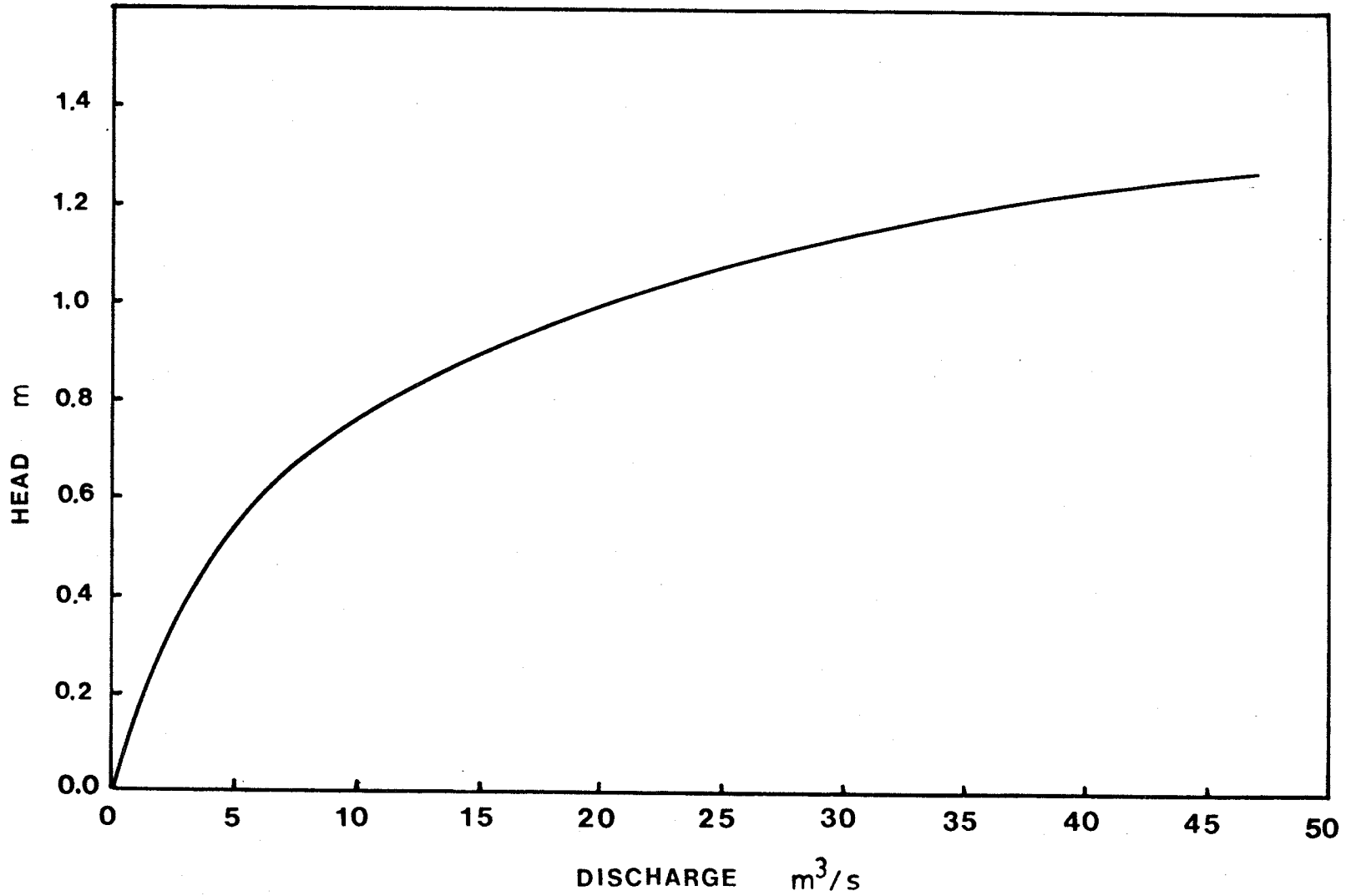
Figure 5.13   HEC-2 Series A - Channel Rating Curve
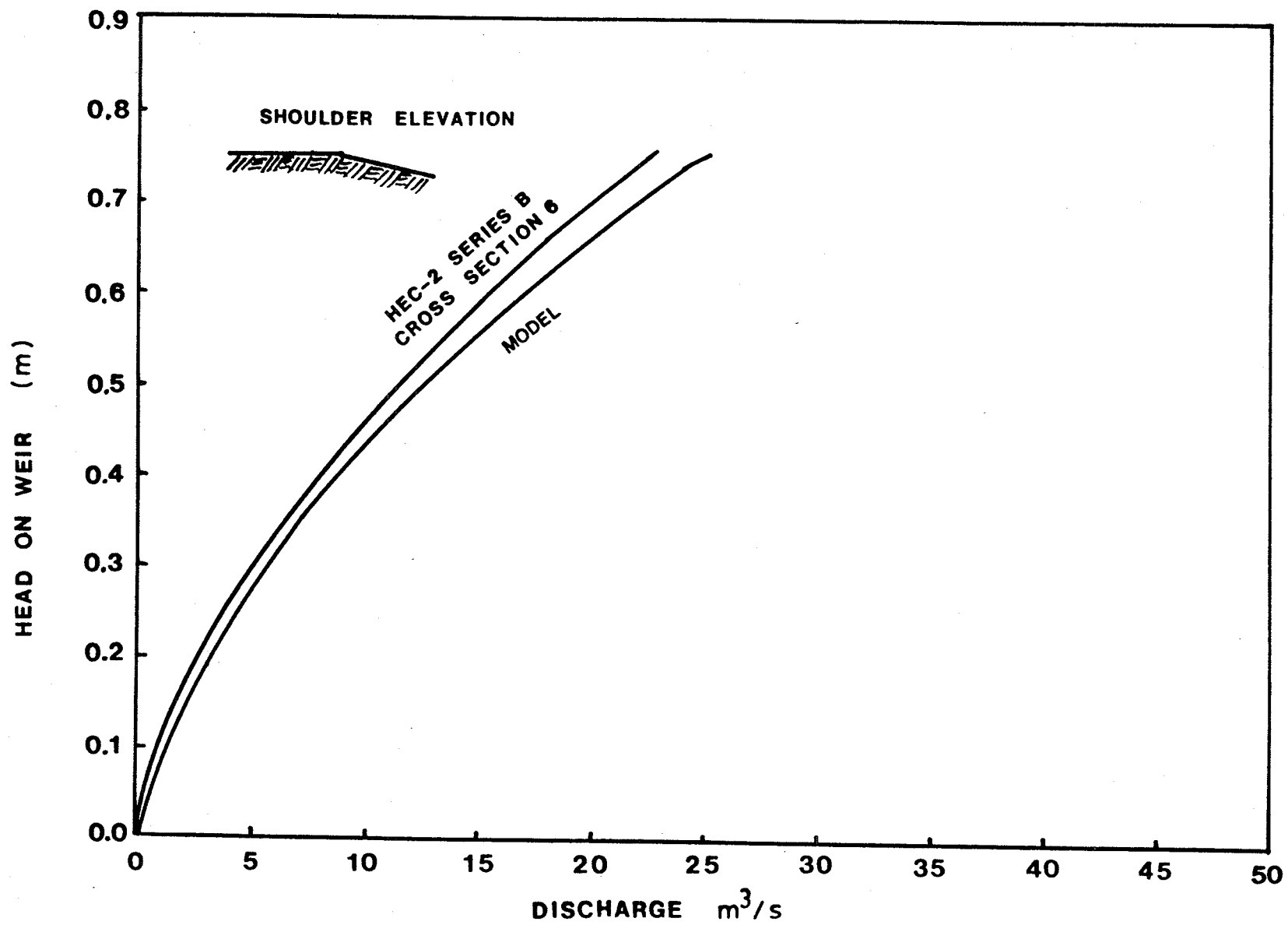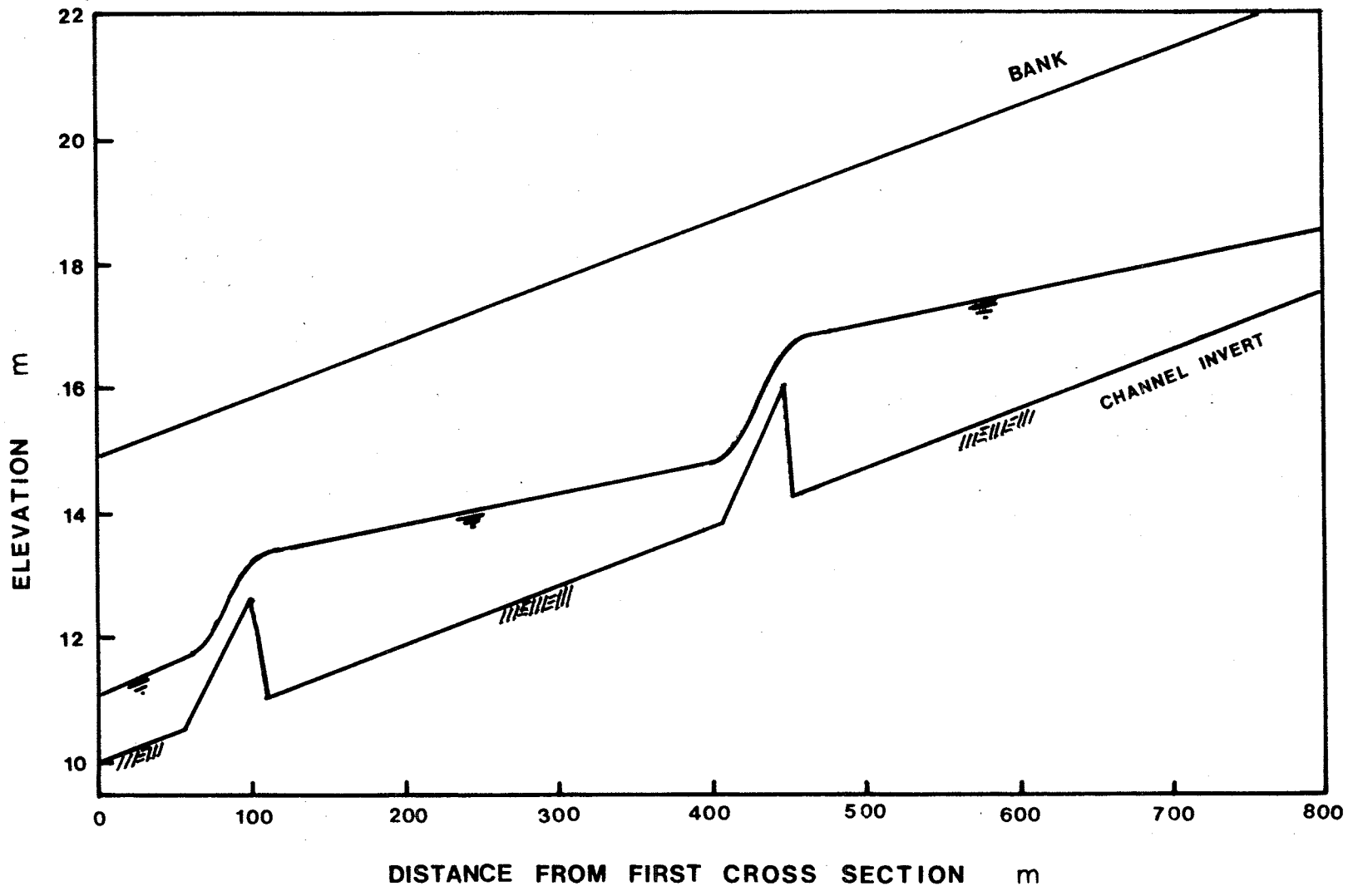
Figure 5.14   HEC-2 Series B – Structure Rating Curve

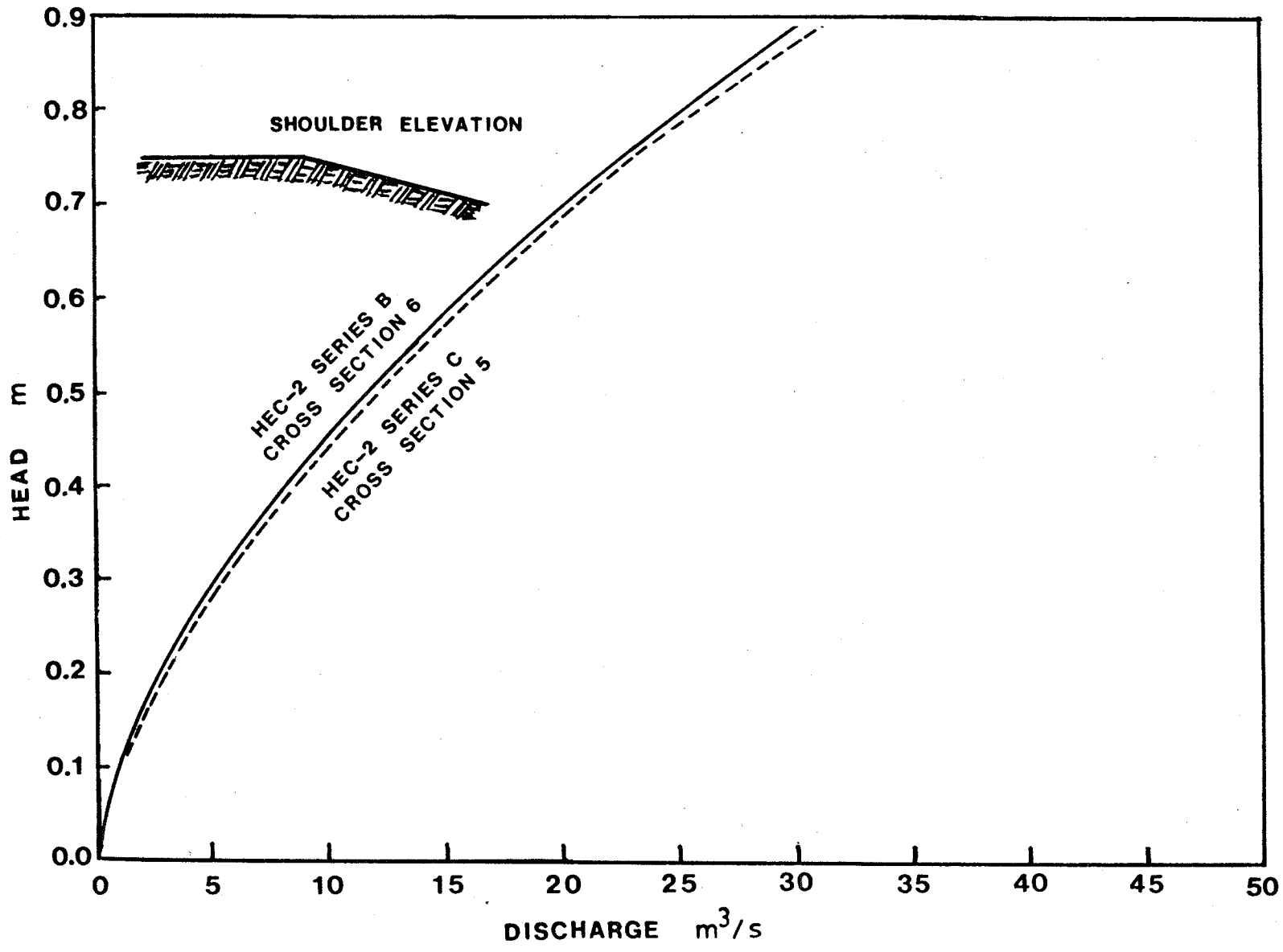Figure 5.15   HEC-2 Series B – Water Surface Profile at Design Discharge

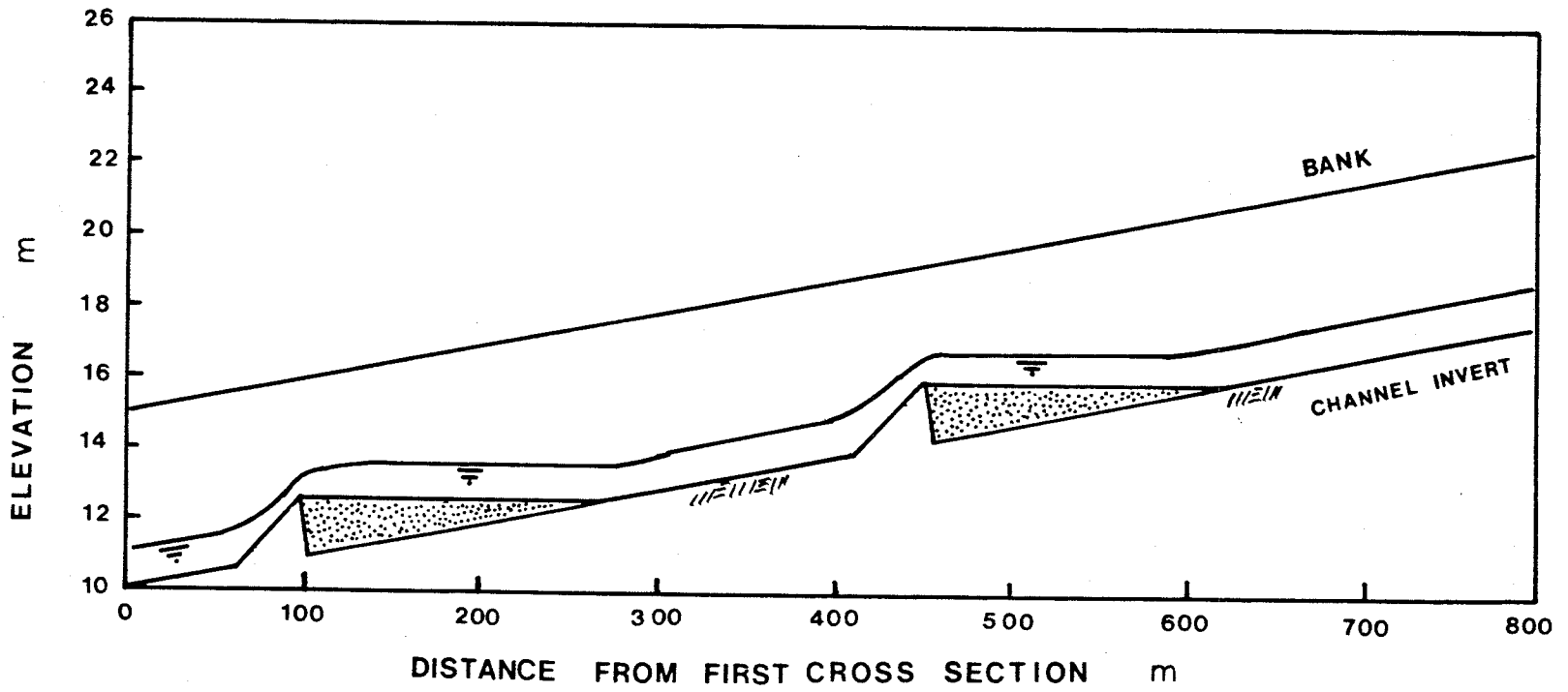Figure 5.16   HEC-2 Series C - Structure Rating Curve

Figure 5.17   HEC 2 Series C – Water Surface Profile at Design Discharge

Appendix B

PLATES

Plate 1   Wilson Creek - Reach through Alluvial Fan

Plate 2   Downstream Prototype Structure - Spring 1981

Plate 3   Pool Upstream of Downstream Prototype Structure Look-
ing Towards Crest – Spring 1981

Plate 4   Dry Pool Upstream of Downstream Prototype Structure
Looking Towards Crest – August 1981

Plate 5   Profile of Downstream Prototype Structure — August
1981

Plate 6   Profile of Upstream Prototype Structure — August 1981

Plate 7   Undistorted Two Dimensional Model Prior to Testing

Plate 8   Silica Sand Bed Downstream of Model Following Testing

Plate 9   Undistorted Three Dimensional Model Prior to Testing

Plate 10   Undistorted Three Dimensional Model at Maximum Discharge

Plate 11   Silica Sand Bed Downstream of Model Following Testing

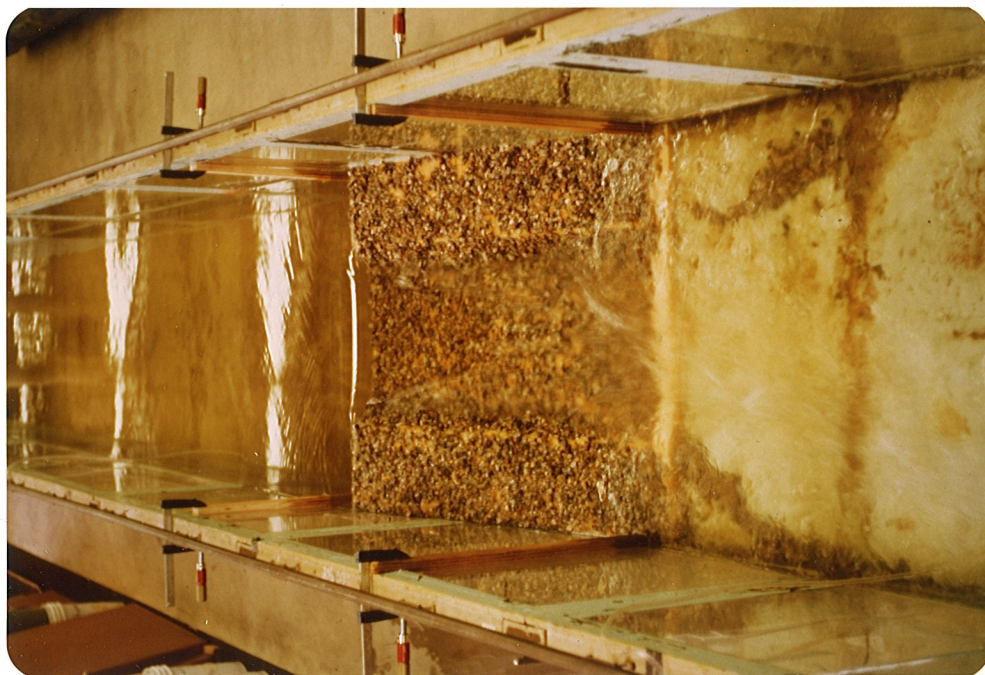Plate 12   Smooth Impermeable Distorted Model at Design Discharge

Plate 13   Roughened Top Layer Permeable Model at Design
             Discharge (d_{50} = 8.5 mm)

Plate 14   Roughened Top Layer Permeable Model at Design
             Discharge (d_{50} = 23 mm)

Plate 15   Roughened Top Layer Permeable Model at Maximum Discharge Tested (d_{50} = 23 mm)

Plate 16   Side View - Roughened Top Layer Permeable Model at Maximum Discharge Tested (d_{50} = 23 mm)
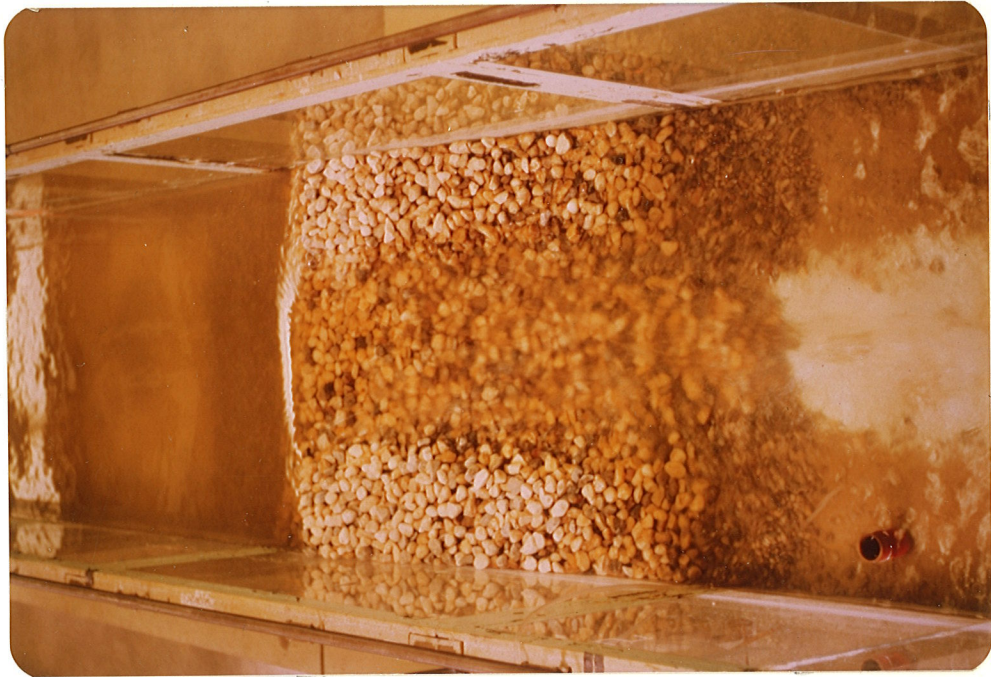
Plate 17   Completely Permeable Model at Design Discharge
(d_{50} = 23 mm)

Plate 18   Side View – Completely Permeable Model at Design
Discharge (d_{50} = 23 mm)